

THE UNIVERSITY OF MICHIGAN
ANN ARBOR, MICHIGAN

QUARTERLY PROGRESS REPORT NO. 8

FOR


BASIC RESEARCH IN MICROWAVE DEVICES AND QUANTUM ELECTRONICS

This report covers the period February 1, 1965 to May 1, 1965

Electron Physics Laboratory
Department of Electrical Engineering

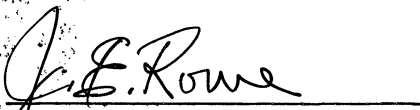
By: M. E. El-Shandwily
B. Ho
J. E. Rowe
C. Yeh

Approved by:



C. Yeh
Project Engineer

Approved by:



J. E. Rowe, Director
Electron Physics Laboratory

Project 05772

DEPARTMENT OF THE NAVY
BUREAU OF SHIPS
WASHINGTON 25, D. C.
PROJECT SERIAL NO. SRO080301, TASK 9391
CONTRACT NO. Nobsr-89274

May, 1965

PN 87

UMR 0567

v. 8

ABSTRACT

Large-signal trajectory computations for a d-c quadrupole amplifier with a twisted quadrafilar pump field structure are presented. Two modes of operation, the cyclotron-to-cyclotron mode and the cyclotron-to-synchronous mode are studied. The results are compared in terms of the paths of electrons for different pump field strength, source of r-f power supply and efficiency. It is believed that the cyclotron-to-synchronous mode of operation is more efficient in many respects.

The derivation of the equation for the V-I characteristic of a tunnel diode is presented. It incorporates the effects of temperature, semiconductor material, doping concentration and the bias voltage on the negative resistance characteristic of the diode. This equation will be used to study cross-modulation effects in the tunnel diode under multiple-input-signal operation.

A small-signal nonlinear analysis of a crossed-field amplifier with n input frequencies is derived. It is found that besides the usual cross-modulation product of frequencies $2f_r - f_p$, as in the case or the O-type TWA, a new product in the form of $f_r + f_p - f_s$ becomes important.

TABLE OF CONTENTS

	<u>Page</u>
ABSTRACT	iii
LIST OF ILLUSTRATIONS	vi
PERSONNEL	vii
1. GENERAL INTRODUCTION	1
2. STUDY OF FREQUENCY MULTIPLICATION IN ANGULAR PROPAGATING CIRCUIT	2
3. ANALYSIS OF AMPLITUDE- AND PHASE-MODULATED TRAVELING- WAVE AMPLIFIERS	2
4. STUDY OF A D-C PUMPED QUADRUPOLE AMPLIFIER	3
4.1 Introduction	3
4.2 Cyclotron-Cyclotron Wave Interaction	3
4.2.1 Low Pump Field	3
4.2.2 High Pump Field	4
4.3 Cyclotron-Synchronous Wave Interaction	8
4.3.1 Nonamplifying Case--Low Pump Field	8
4.3.2 Amplifying Case--High Pump Field	12
4.4 Energy Relations	12
4.5 Conclusion	16
4.6 Future Work	19
5. INVESTIGATION OF THE CROSS-MODULATION PRODUCTS IN A WIDEBAND TUNNEL DIODE AMPLIFIER	19
5.1 The Quantum Mechanical Tunneling Effect	19
5.2 The Tunnel Diode	24
5.3 The V-I Characteristic	26
5.4 An Approximate Solution of the V-I Characteristic	33
5.5 Future Work	36

	<u>Page</u>
6. NONLINEAR ANALYSIS OF THE CROSSED-FIELD AMPLIFIER WITH MULTI-SIGNAL INPUT	37
6.1 Introduction	37
6.2 Theoretical Analysis	37
6.3 Future Work	58
7. GENERAL CONCLUSIONS	58

LIST OF ILLUSTRATIONS

<u>Figure</u>		<u>Page</u>
4.1	Cyclotron-Cyclotron Wave Interaction for Low Pump Field Strength.	5
4.2	Electron Trajectory of Different Entrance Angle for Cyclotron-Cyclotron Wave Interaction and Low Pump Field.	6
4.3	Cyclotron-Cyclotron Wave Interaction for High Pump Field Strength.	7
4.4	Cyclotron-Synchronous Wave Interaction for Very Low Pump Field Strength. ($V_p = 10$ Volts)	9
4.5	Cyclotron-Synchronous Wave Interaction for Low Pump Field Strength. ($V_p = 30$ Volts)	10
4.6	Cyclotron-Synchronous Wave Interaction for Low Pump Field Strength. ($V_p = 42$ Volts)	11
4.7	Cyclotron-Synchronous Wave Interaction for High Pump Field Strength. ($V_p = 53$ Volts)	13
4.8	Angular Variation for Different Pump Field Strengths.	14
4.9	Energy Variation of Cyclotron-Cyclotron Wave Interaction.	17
4.10	Energy Variation of Cyclotron-Synchronous Wave Interaction.	18
5.1	Quantum Mechanical Tunneling.	21
5.2	The V-I Characteristic of a Typical Tunnel Diode.	25
5.3	Energy Level Diagram of a Tunnel Diode.	27
5.4	Energy Level Diagram, Density of States and the Definition of Terms Used in Analyzing the V-I Characteristics of a Tunnel Diode.	28
5.5	The Density of States Function for a Degenerate N-Type Semiconductor Showing the Effect of Broadening of the Impurity Level E_D .	32

PERSONNEL

<u>Scientific and Engineering Personnel</u>		<u>Time Worked in</u> <u>Man Months*</u>
J. Rowe	Professors of Electrical Engineering	.05
C. Yeh		1.11
D. Solomon	Associate Research Engineer	.51
H. Detweiler	Assistant Research Engineers	.97
W. Rensel		.11
M. El-Shandwily	Research Associate	2.93
A. Cha	Research Assistants	1.66
A. Heath		.55
B. Ho		1.27
R. Ying		1.59
<u>Service Personnel</u>		8.40

* Time Worked is based on 172 hours per month.

QUARTERLY PROGRESS REPORT NO. 8

FOR

BASIC RESEARCH IN MICROWAVE DEVICES AND QUANTUM ELECTRONICS

1. General Introduction (C. Yeh)

The broad purpose of this project is to investigate new ideas in the area of microwave devices and quantum electronics. The program is envisioned as a general and flexible one under which a wide variety of topics may be studied. At present, the following areas of investigation are in progress:

A. Study of frequency multiplication in an angular propagating structure. Fabrication of a low-frequency multiplier tube which multiplies a 600 mc input signal to a 2400 mc output signal with adjustable feedback control is in progress and extensive testing will follow.

B. Analysis of amplitude- and phase-modulated traveling-wave amplifiers. This phase of the investigation has been concluded and a final summary on the experimental findings will be given.

C. Study of a d-c pumped quadrupole amplifier. Electron trajectories in a d-c pumped quadrupole structure are computed by solving the equations of motion for different modes of interaction. From the computer results on trajectories energy relations will be derived and studied.

D. Investigation of the cross-modulation products in a wideband tunnel diode amplifier. Theoretical expressions for the voltage-current characteristic of a forward biased tunnel diode will be derived, linking

the effects of temperature, doping concentration and the bias voltage to the characteristics. The portion of the characteristic which shows the negative resistance will be used to compute the cross-modulation effects when multiple signal inputs are applied.

E. Nonlinear analysis of the crossed-field amplifier with multi-frequency input signals. A study of the nonlinear beam-circuit interaction in the M-type amplifier will be conducted for small multi-frequency input signals. The output spectrum will contain frequencies not present at the input. Equations for the output spectrum will be derived and computed.

2. Study of Frequency Multiplication in Angular Propagating Circuit

(C. Yeh and B. Ho)

The work on fabrication of the experimental low-frequency multiplier tube is progressing. A quadrupole helix with reasonable uniformity has been successfully wound by inserting the wires in the grooves cut on the supporting sapphire rods.

Cuccia couplers of proper dimensions have been mounted on both ends of the cavity and inductances have been added to tune them to proper frequencies. A method of coupling an r-f signal into the coupler has been worked out. It consists of a coupling loop located outside of the envelope to affect the coupling inductively.

3. Analysis of Amplitude- and Phase-Modulated Traveling-Wave Amplifiers

(M. E. El-Shandwily and J. E. Rowe)

A summary technical report on the nonlinear operation of the traveling-wave amplifier with multi-signal input has been written. The computer results for the large-signal analysis which have not been

reported in the previous reports are included. It also contains all the available information concerning this problem. It is expected that the report will be issued during the next period.

4. Study of a D-c Pumped Quadrupole Amplifier (C. Yeh and B. Ho)

4.1 Introduction. The equations of motion for the cyclotron-cyclotron wave interaction and cyclotron-synchronous wave interaction of a d-c pumped quadrupole amplifier have been developed in Interim Scientific Reports No. 5 and No. 6 respectively.

During this period, the computer solution of these equations for various initial conditions has been obtained. The results are presented in the form of electron trajectories and energies. Some of these data will be plotted and discussed in this report.

The computations are based upon the following pump structure constants:

Cyclotron frequency	1200 mc
Helix pitch	8.4 mm
Helix radius	1 mm
Magnetic field	430 gauss
Beam voltage	300 volts

4.2 Cyclotron-Cyclotron Wave Interaction. Under this condition, the electron trajectories and energy relations for two different pump fields are studied.

4.2.1 Low Pump Field. For the particular pump field structure under consideration, a pump voltage of less than 15 volts

can be considered as a very low pump field. The reason for choosing this value will be made clear later.

The results of the solution can best be interpreted by plotting the relative motion of the electron with respect to the pump field. Figures 4.1 and 4.2 show the trajectories of electrons for different pump field strengths in relation to a stationary pump field. The trajectories for low pump field strengths are all of similar shape. Their radius of rotation increases with time after they enter the pump field structure, reaches a maximum approximately along a 45-degree line and then decreases. It will be clear in the next section that the 45-degree line, where the positive helix wire is located, is the line which separates the amplifying and nonamplifying regions.

In Fig. 4.1 only the trajectories of the most favorably phased electrons are plotted. However, in order to show the phase-focusing effect for the unfavorable electrons after their entrance, a plot of trajectories for different entrance phases under the same pumping voltage is given in Fig. 4.2. It can be seen that electrons entering at all angles will slip into the trajectories of the most favorably phased ones within a few cyclotron periods after entrance. Eventually, they group into two spokes.

4.2.2 High Pump Field. When the pump voltage is raised, the shape of the trajectory changes. The electron tends to move toward the positive helix wire. Consequently, the radius of rotation increases monotonically with time. Figure 4.3 shows some of these trajectories. It is noticed that the increase of the radius of rotation is along a

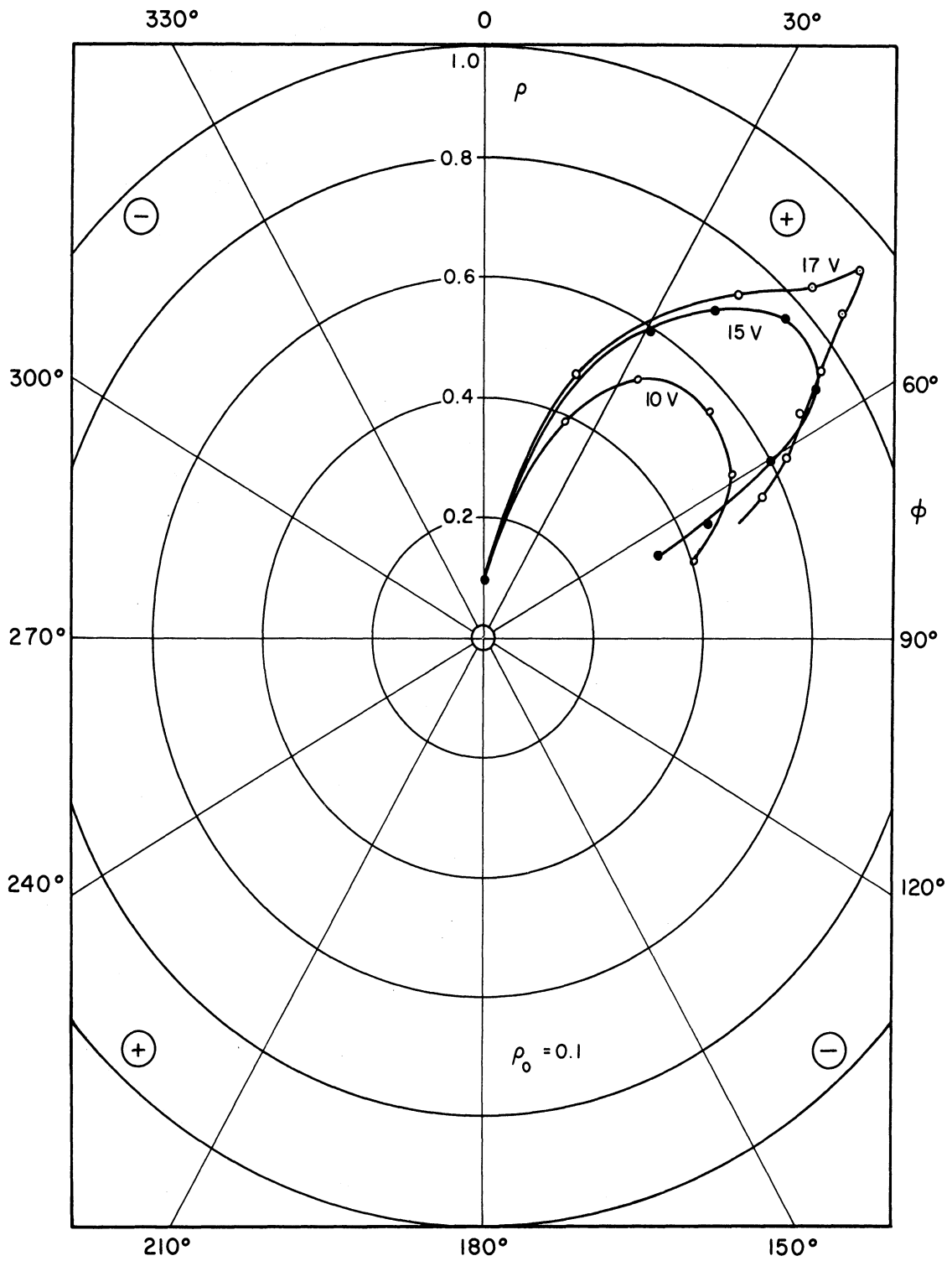


FIG. 4.1 CYCLOTRON-CYCLOTRON WAVE INTERACTION FOR LOW PUMP FIELD STRENGTH.

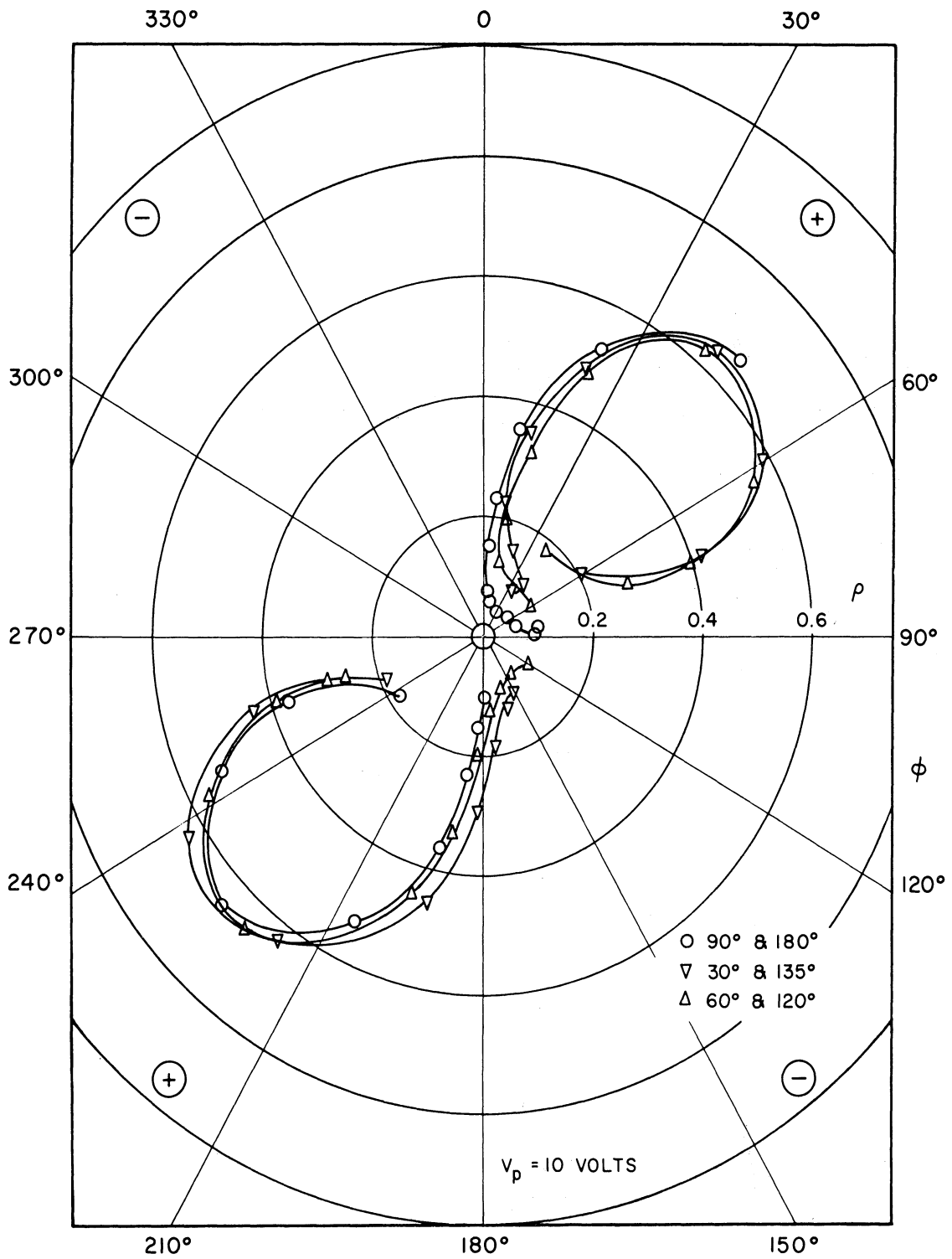
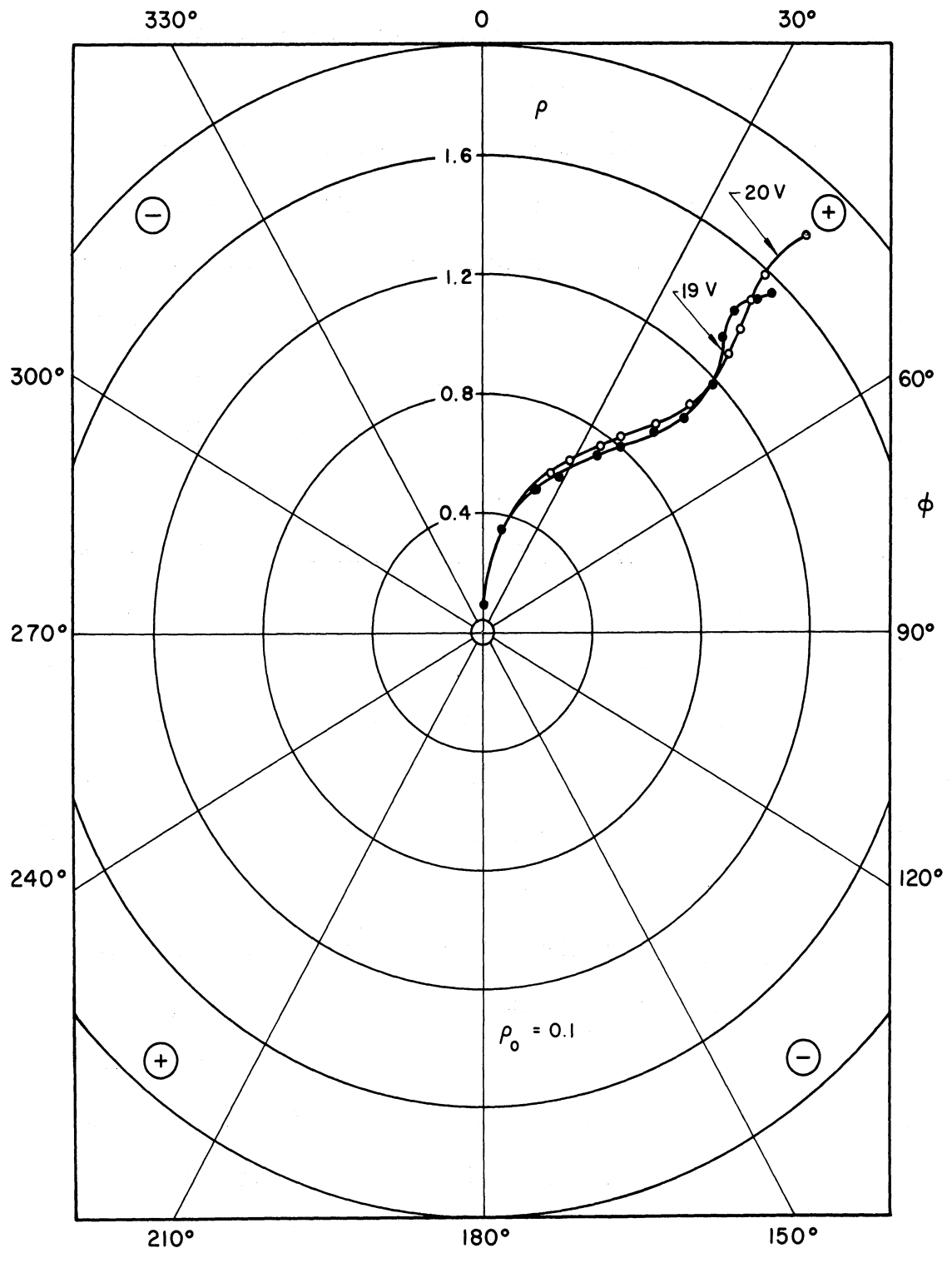


FIG. 4.2 ELECTRON TRAJECTORY OF DIFFERENT ENTRANCE ANGLE FOR CYCLOTRON-CYCLOTRON WAVE INTERACTION AND LOW PUMP FIELD.



straight line approximately 45 degrees from the reference line. This is the location of the positive helix wire.

An increase in radius of rotation signifies that the rotational energy of the electron has been increased. If useful energy can be derived from this electron, amplification or gain results. It can be seen from Fig. 4.3 that amplifying electrons stay above the 45-degree line while the nonamplifying electrons reach a maximum at or around the 45-degree line and then decrease in radius of rotation (see Figs. 4.1 and 4.2).

4.3 Cyclotron-Synchronous Wave Interaction. The pump field structure used for this study is the same as in the case of cyclotron-cyclotron wave interaction. However, the beam voltage is reduced to one fourth as much to satisfy the requirement for this type of wave interaction, i.e., $\beta_q = 1/2 \beta_c$ (see Interim Scientific Reports No. 5 and No. 6). Two cases have been studied; the nonamplifying case and the amplifying case.

4.3.1 Nonamplifying Case--Low Pump Field. When the pump voltage is smaller than the critical value, i.e., $V_p < V_o (\beta_c a)^2/4$, the pump field has very little effect upon the trajectory of the beam electrons. The beam keeps rotating at the cyclotron frequency while the pump field rotates at half of the cyclotron frequency. Figure 4.4 shows the trajectories for a very low pump field. A stationary pump field is assumed in this plot. Under this pump field strength, the radius of rotation decreases as the beam moves along, and thus no gain can be obtained. As the pump field strength increases, the effect of the pump field becomes noticeable. This is shown in Figs. 4.5 and 4.6.

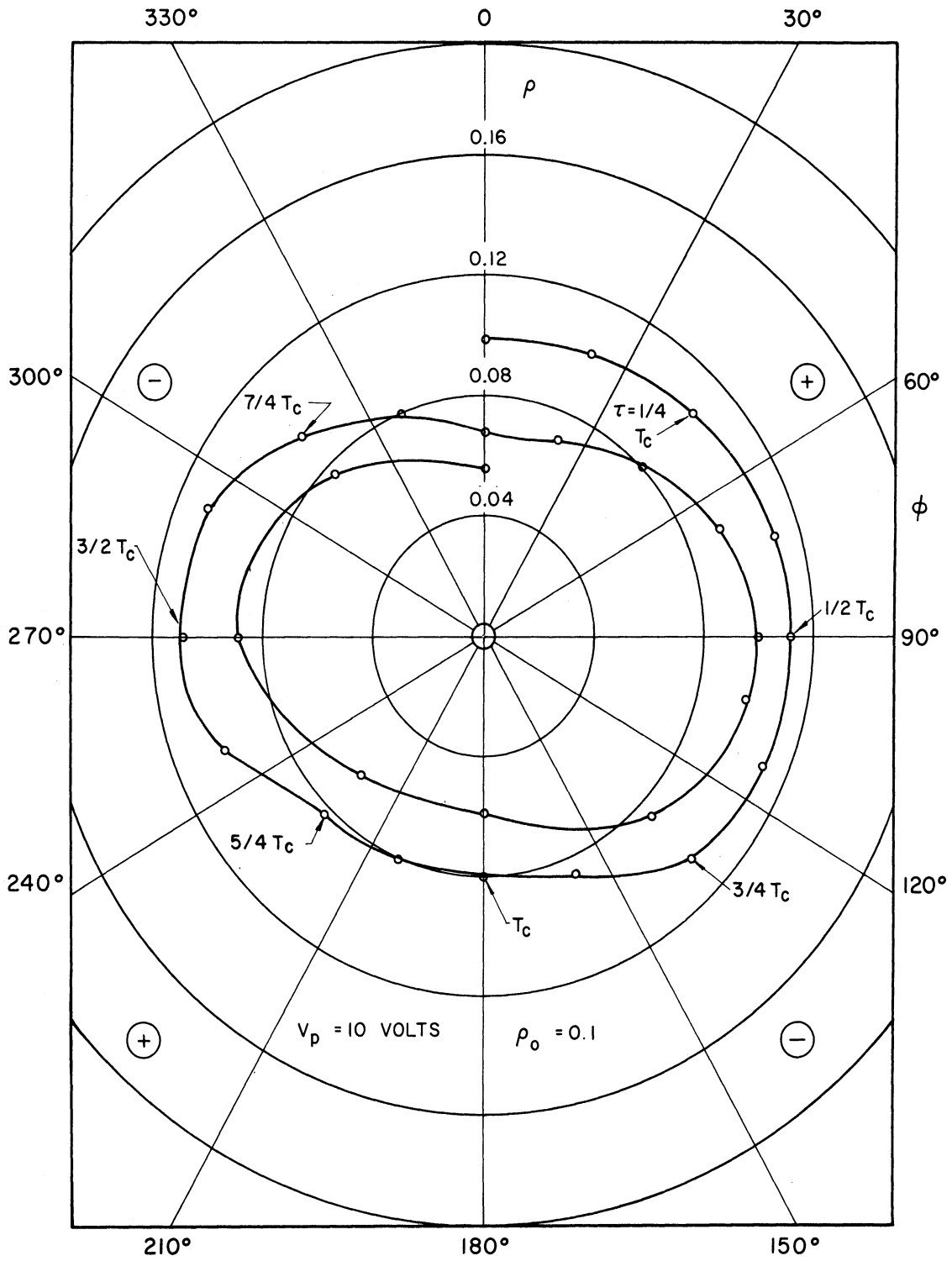


FIG. 4.4 CYCLOTRON-SYNCHRONOUS WAVE INTERACTION FOR VERY LOW PUMP FIELD STRENGTH. ($V_p = 10$ VOLTS)

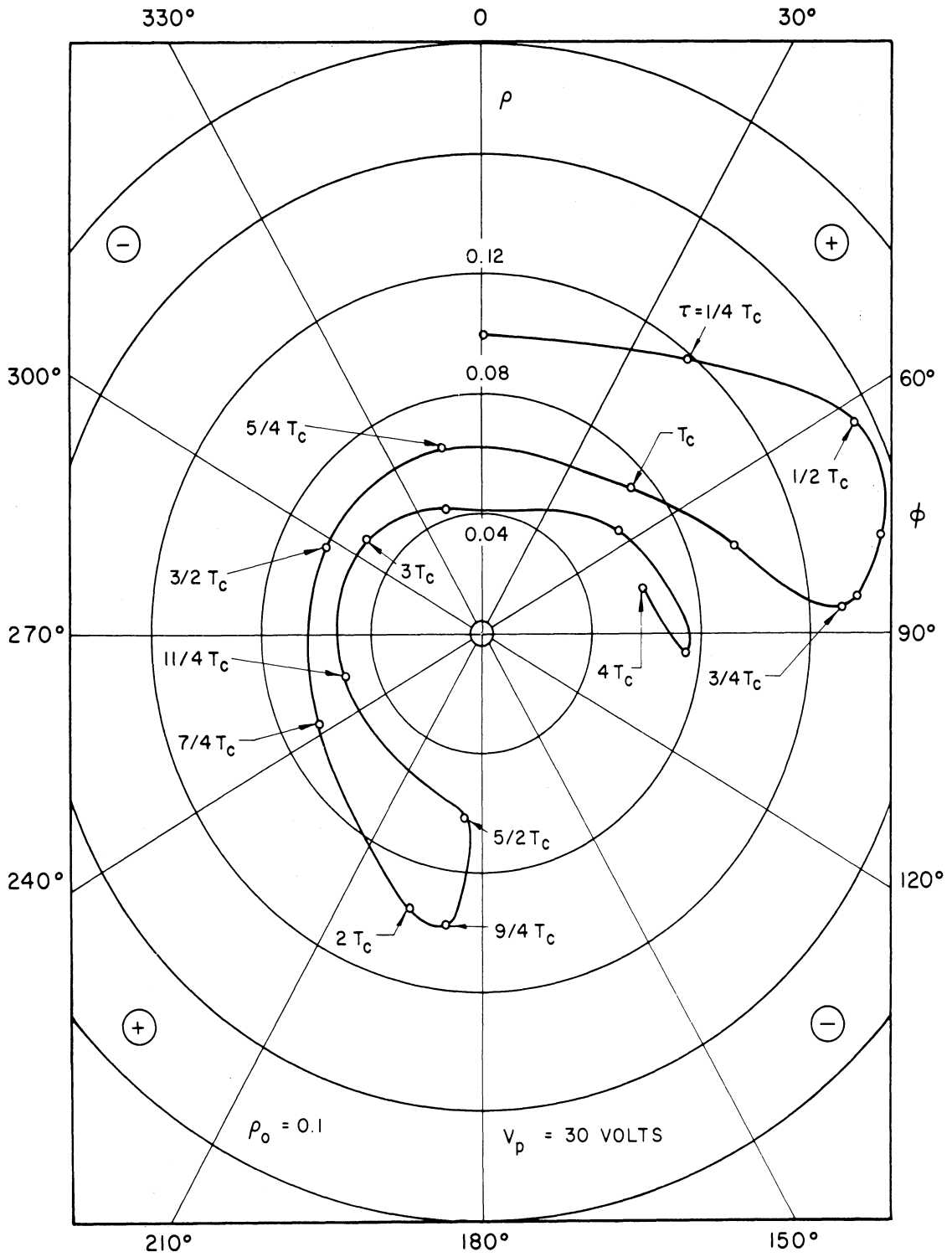


FIG. 4.5 CYCLOTRON-SYNCHRONOUS WAVE INTERACTION FOR LOW PUMP FIELD STRENGTH. ($V_p = 30$ VOLTS)

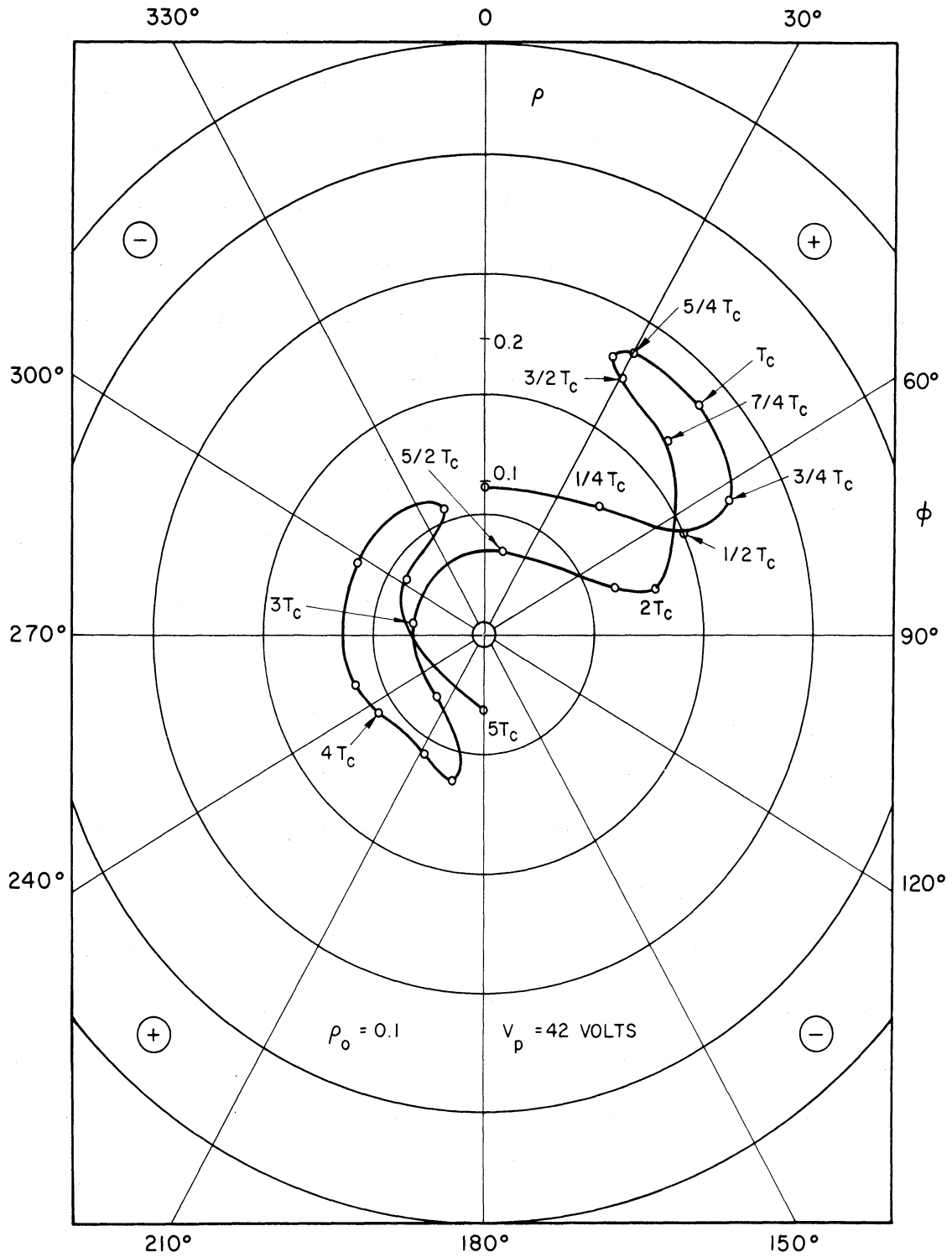


FIG. 4.6 CYCLOTRON-SYNCHRONOUS WAVE INTERACTION FOR LOW PUMP FIELD STRENGTH. ($V_p = 42$ VOLTS)

4.3.2 Amplifying Case--High Pump Field. When the pump voltage is raised above the critical value, the pump field gains control over the motion of the beam. After entering into the pump field structure, the electron beam starts to retard in phase and lock into step with the pump field. The radius of rotation increases as the electrons gain energy from the pump field. Gain is therefore obtained in this case. Figure 4.7 shows two of those trajectories. Equipotential lines of the pump field structure are also drawn in the figure to show how the electron gains energy during its course of motion.

The angular displacement of the beam electrons for both cases are plotted in Fig. 4.8. The slope of the curve shows that the beam rotates at a rate equal to the cyclotron frequency for the nonamplifying case, while in the amplifying case the beam rotates at the cyclotron frequency at the beginning, but it starts to slow down and finally rotates at half of the cyclotron frequency, which is the same rate as the pump field.

4.4 Energy Relations. It is generally believed that the transverse energy of the rotating beam of a d-c quadrupole amplifier is converted from the axial energy of the beam. In other words, the r-f power is amplified at the expense of the axial beam power. As the beam passes along the pump field structure, the beam velocity would decrease. This energy conversion process gives rise to the problem of synchronization between the beam waves and the pump field. The problem becomes more serious especially if the device is operated at a large-signal level. As has been shown in Interim Scientific Report No. 6, for a phase slip of more than 45 degrees, the beam will fall into the attenuation region and gain is sharply decreased. Because of this

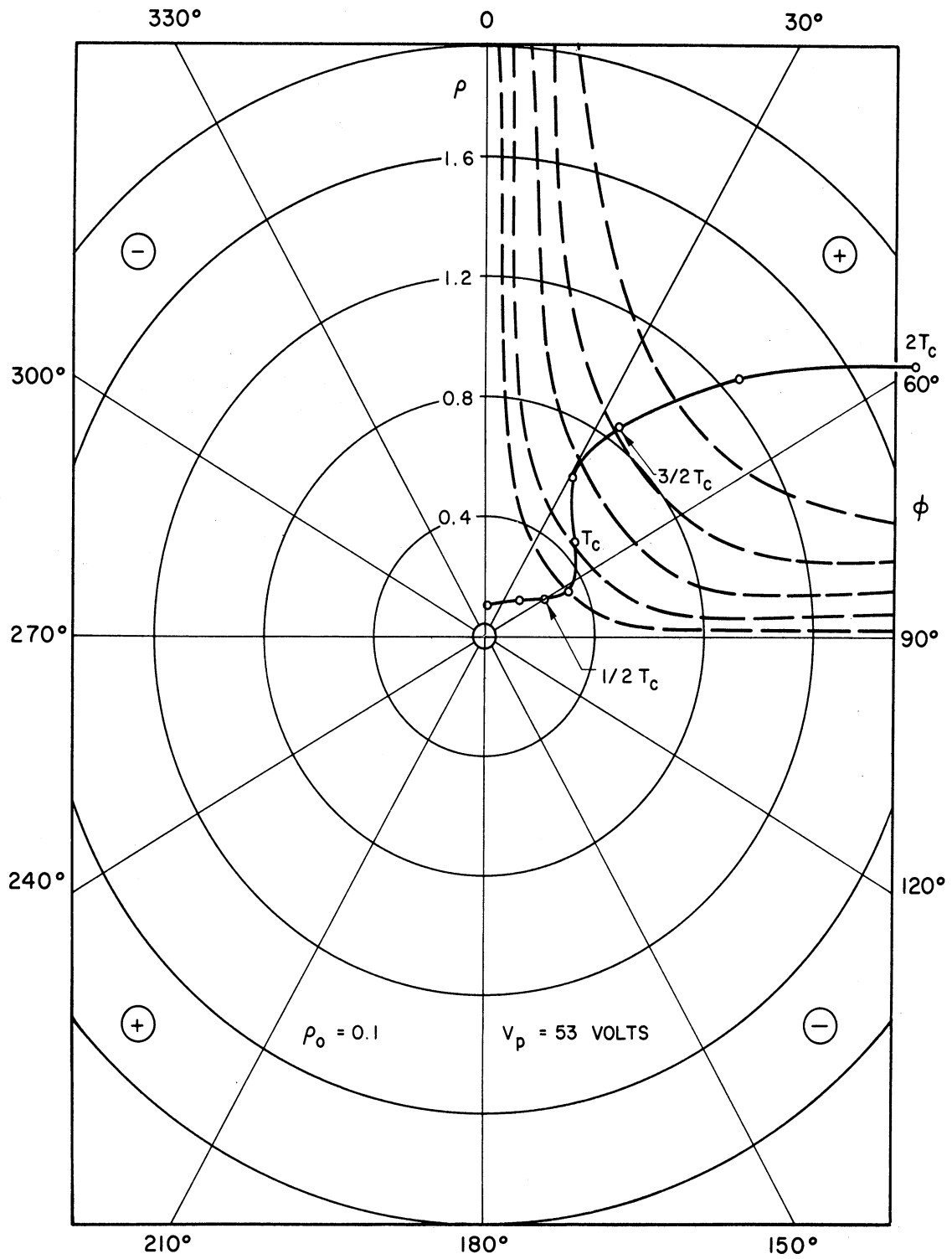


FIG. 4.7 CYCLOTRON-SYNCHRONOUS WAVE INTERACTION FOR HIGH PUMP FIELD STRENGTH. ($V_p = 53$ VOLTS)

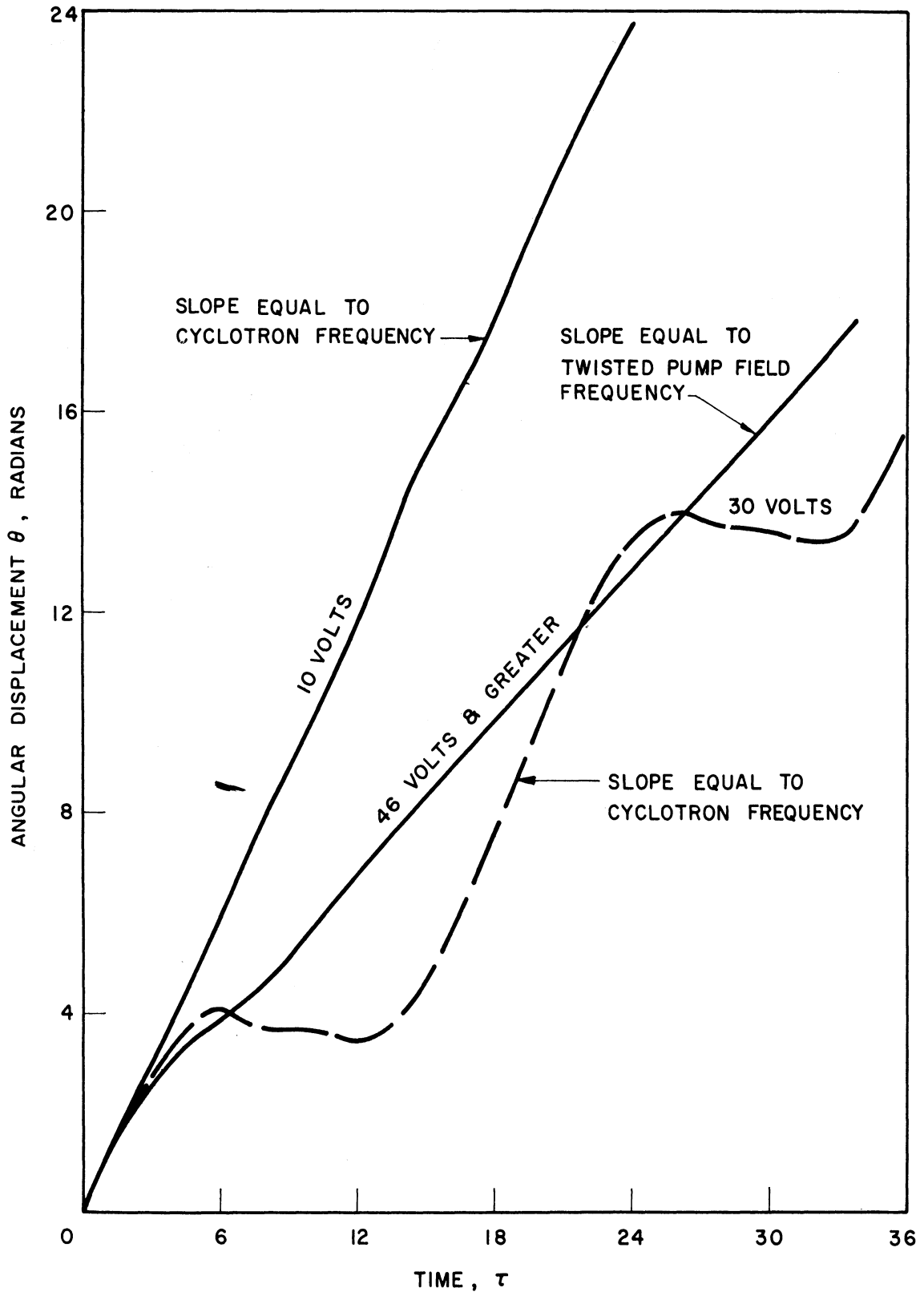


FIG. 4.8 ANGULAR VARIATION FOR DIFFERENT PUMP FIELD STRENGTHS.

inherent difficulty, the overall efficiency of this type of device is comparatively low at a theoretical maximum of 33 percent even with depressed collector operation¹.

From the energy relation study of the computer solution it can be shown that under some beam-wave interactions, the axial velocity remains almost constant. This indicates that the transverse energy of the rotating beam must come from the pump field. This is contrary to the common belief. If this is true, then the off-synchronization problem would no longer exist. Consequently, a high efficiency transverse wave amplifier is thus possible. The anomalous gain mechanism reported previously belongs to this type of interaction.

Let us now evaluate the energy balance relations. In Interim Scientific Report No. 6, the transverse energy in terms of the radial displacement ρ , angular displacement Φ , was given as

$$E_{\text{trans}} = E_{\text{rad}} + E_{\text{tan}} ,$$

where

$$E_{\text{rad}} = eV_0 \dot{\rho}^2$$

and

$$E_{\text{tan}} = eV_0 \rho^2 (1 + \dot{\Phi})^2 .$$

The axial energy is given by

$$E_{\text{axial}} = eV_0 \dot{\xi}^2 .$$

1. Curnow, H. J., "The Efficiency of Electrostatic Quadrupole Amplifiers", Jour. Elect. and Control, vol.11, pp. 161-176; September, 1961.

The computer solution for the energies in the cyclotron-cyclotron wave interaction is given in Fig. 4.9. It can be seen that as the radius of rotation increases the axial energy decreases rapidly. This conforms with the general belief that energy is derived from axial energy. However, when the device is operated at a very large signal level, ρ approaches unity and the total energy exceeds the initial beam energy, which means that even in cyclotron-cyclotron wave interaction an energy transfer from pump field to the beam would also occur.

Figure 4.10 shows the energy variation for the cyclotron-synchronous wave interaction. Notice that the axial energy is essentially constant during the entire amplifying process, while the tangential and radial energy grow as indicated. This result definitely indicates that the transverse energy is coming entirely from the pump field. Another point of interest is that the magnitude of the radial component is much smaller than the tangential component. This indicates that it would give a high efficiency operation since the amplified output is taken from a Cuccia coupler which depends on the tangential component only. Comparing this with Fig. 4.9, it is obvious that the cyclotron-synchronous mode of operation is more efficient.

4.5 Conclusion. From the computer study of the transverse wave amplifier, the exact trajectory of the electron is known. From this the gain of the interaction can also be determined. This condition as well as the amount of interaction obtained from this computer study is entirely in agreement with the coupled-mode analysis given in Interim Scientific Report No. 3. The most significant point obtained from this study is the understanding of the energy relation for various

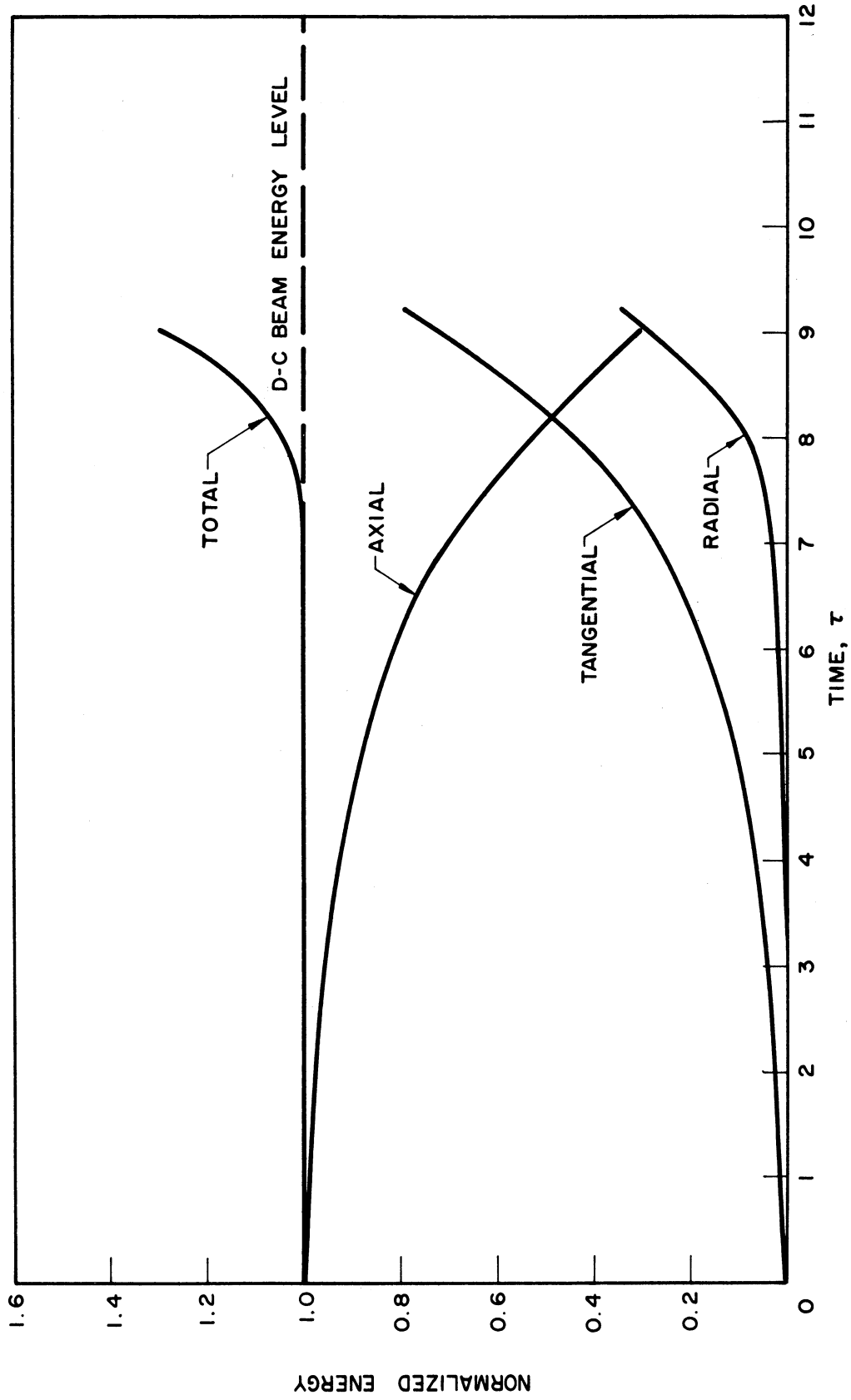


FIG. 4.9 ENERGY VARIATION OF CYCLOTRON-CYCLOTRON WAVE INTERACTION.

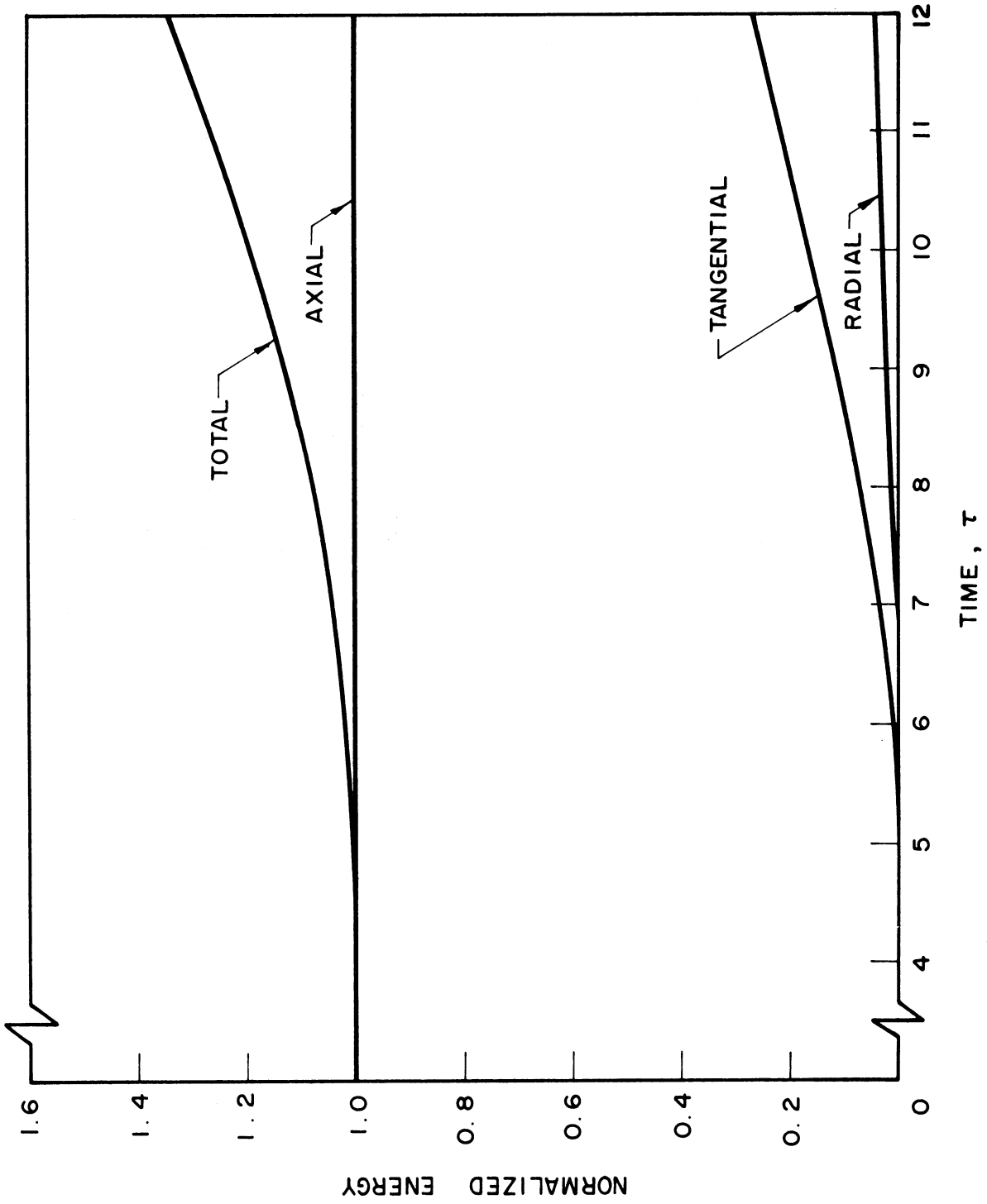


FIG. 4.10 ENERGY VARIATION OF CYCLOTRON-SYNCHRONOUS WAVE INTERACTION.

modes of interaction. It is contrary to the general belief that the d-c pump could possibly feed energy to the orbiting electron. With the conventional concept of axial-transverse energy conversion, the efficiency is limited to a low value; however, with this pump-transverse energy conversion, a high efficiency device of this type is entirely possible.

4.6 Future Work. It seems quite feasible that a high power, high efficiency d-c quadrupole amplifier can be designed. The elements involved would be simple and the construction would be simple. It is the intention of the authors to try this approach.

5. Investigation of the Cross-Modulation Products in a Wideband Tunnel Diode Amplifier (C. Yeh)

5.1 The Quantum Mechanical Tunneling Effect. The time-invariant Schrödinger wave equation can be expressed in the form

$$\nabla^2\psi + \frac{2m}{\hbar^2} (E - U) \psi = 0 , \quad (5.1)$$

where ψ is the probability density function such that

$$\int_V \psi\psi^* dV = 1 ,$$

or in other words that the amplitude of ψ squared, when properly normalized, indicates the probability of finding a particle in the volume. E is the total energy, U is the potential energy and $\hbar = h/2\pi$ where h is Planck's constant. The term $E - U$ represents the kinetic energy.

Whereas in classical mechanics a negative kinetic energy is not permitted, it is allowable in quantum theory. In fact the solution of Eq. 5.1 under the condition that $E - U < 0$ is fundamental to the theory of tunneling.

Assume that one has a potential barrier U_0 in a one-dimensional space, and that the particle energies are less than U_0 as shown in Fig. 5.1. The solutions to the wave equations in the three regions are, respectively, for $x < 0$,

$$\psi_1 = A \exp\left(j \frac{p_1 x}{\hbar}\right) + B \exp\left(-j \frac{p_1 x}{\hbar}\right), \quad (5.2)$$

for $0 < x < x_1$,

$$\psi_2 = C \exp\left(\frac{p_2 x}{\hbar}\right) + D \exp\left(\frac{-p_2 x}{\hbar}\right), \quad (5.3)$$

and for $x > x_1$

$$\psi_3 = F \exp\left(j \frac{p_1 x}{\hbar}\right), \quad (5.4)$$

where

$$p_1 = \sqrt{2mE},$$
$$p_2 = \sqrt{2m(U_0 - E)}.$$

The boundary conditions are that the functions ψ_1 , ψ_2 and ψ_3 and their derivatives $\partial\psi_1/\partial x$, $\partial\psi_2/\partial x$ and $\partial\psi_3/\partial x$ must be continuous at $x = 0$ and $x = x_0$ respectively. These conditions enable one to solve for four out of five arbitrary constants. Thus one should be able to express any four of these arbitrary constants in terms of the fifth one. Thus

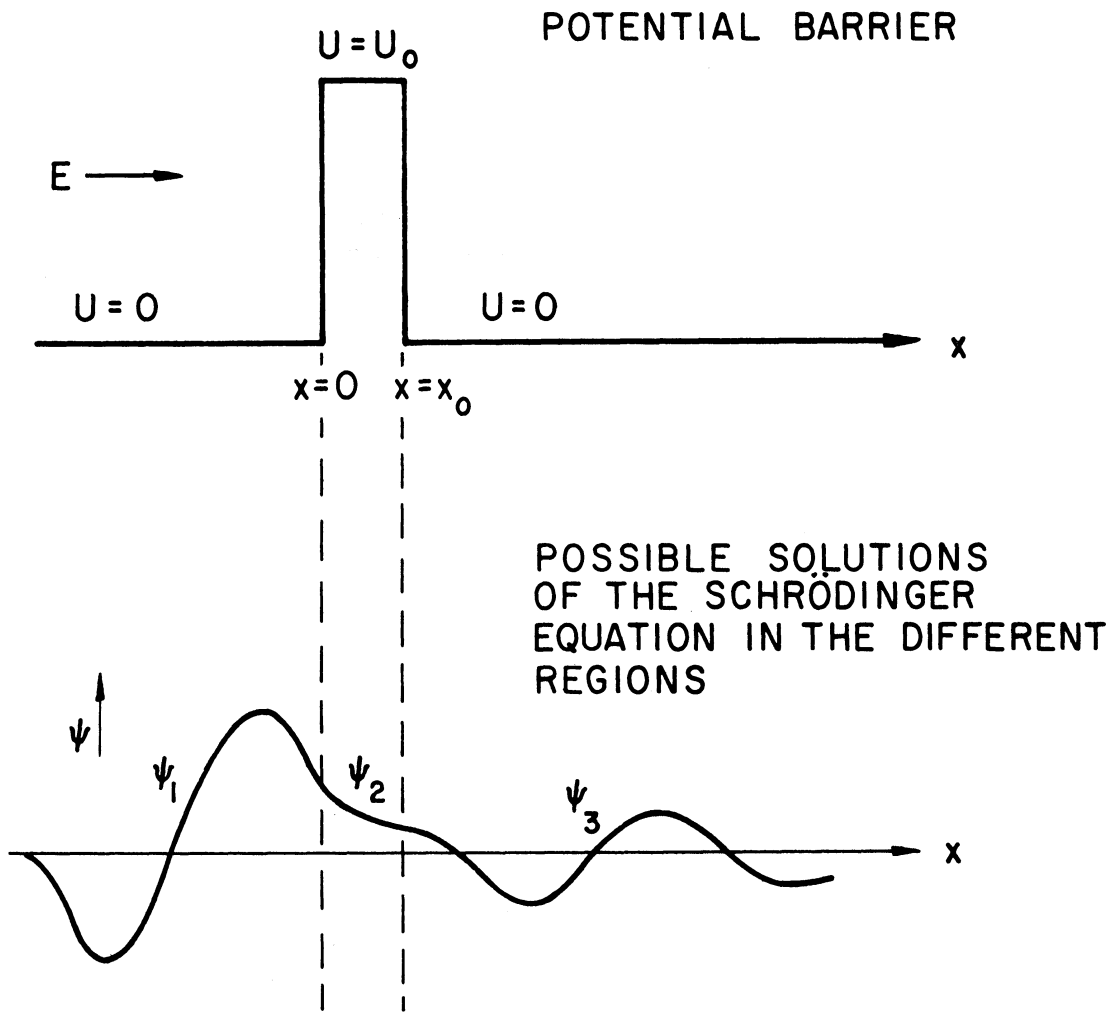


FIG. 5.1 QUANTUM MECHANICAL TUNNELING.

$$\psi_1(0) = A + B ,$$

$$\psi_2(0) = C + D ,$$

$$\psi_2(x_0) = C \exp\left(\frac{p_2 x_0}{\hbar}\right) + D \exp\left(\frac{-p_2 x_0}{\hbar}\right) \text{ and}$$

$$\psi_3(x_0) = F \exp\left(j \frac{p_1 x_0}{\hbar}\right)$$

$$\left. \frac{\partial \psi_1}{\partial x} \right|_0 = j \frac{p_1}{\hbar} A - j \frac{p_1}{\hbar} B ,$$

$$\left. \frac{\partial \psi_2}{\partial x} \right|_0 = \frac{p_2}{\hbar} C - \frac{p_2}{\hbar} D ,$$

$$\left. \frac{\partial \psi_2}{\partial x} \right|_{x_0} = \frac{p_2}{\hbar} C \exp\left(\frac{p_2 x_0}{\hbar}\right) - \frac{p_2}{\hbar} D \exp\left(-\frac{p_2 x_0}{\hbar}\right) \text{ and}$$

$$\left. \frac{\partial \psi_3}{\partial x} \right|_{x_0} = j \frac{p_1}{\hbar} F \exp\left(j \frac{p_1 x_0}{\hbar}\right) .$$

Then

$$A + B = C + D$$

$$C \exp\left(\frac{p_2 x_0}{\hbar}\right) + D \exp\left(-\frac{p_2 x_0}{\hbar}\right) = F \exp\left(j \frac{p_1 x_0}{\hbar}\right)$$

$$j \frac{p_1}{\hbar} A - j \frac{p_1}{\hbar} B = \frac{p_2}{\hbar} C - \frac{p_2}{\hbar} D$$

$$\frac{p_2}{\hbar} C \exp\left(\frac{p_2 x_0}{\hbar}\right) - \frac{p_2}{\hbar} D \exp\left(-\frac{p_2 x_0}{\hbar}\right) = j \frac{p_1}{\hbar} F \exp\left(j \frac{p_1 x_0}{\hbar}\right) .$$

If A, B, C and D are solved in terms of F, one obtains

$$\begin{aligned}
 A &= \frac{F}{4} \left\{ \left(1 - j \frac{p_1}{p_2}\right) \left(1 + j \frac{p_2}{p_2}\right) \exp \left[(jp_1 + p_2) \frac{x_0}{\hbar} \right] \right. \\
 &\quad \left. + \left(1 + j \frac{p_1}{p_2}\right) \left(1 - j \frac{p_2}{p_1}\right) \exp \left[(jp_1 - p_2) \frac{x_0}{\hbar} \right] \right\} , \\
 B &= \frac{F}{4} \left\{ \left(1 - j \frac{p_1}{p_2}\right) \left(1 - j \frac{p_1}{p_2}\right) \exp \left[(jp_1 + p_2) \frac{x_0}{\hbar} \right] \right. \\
 &\quad \left. + \left(1 + j \frac{p_2}{p_1}\right) \left(1 + j \frac{p_1}{p_2}\right) \exp \left[(jp_1 - p_2) \frac{x_0}{\hbar} \right] \right\} , \\
 C &= \frac{F}{2} \left(1 + j \frac{p_1}{p_2}\right) \exp \left[(jp_1 - p_2) \frac{x_0}{\hbar} \right] , \\
 D &= \frac{F}{2} \left(1 - j \frac{p_1}{p_2}\right) \exp \left[(jp_1 + p_2) \frac{x_0}{\hbar} \right] .
 \end{aligned} \tag{5.5}$$

If one defines a transmission coefficient T as the ratio of the power of the transmitted to incident waves, then

$$T = \frac{|F|^2}{|A|^2} = \frac{1}{\cosh^2 \left(p_2 \frac{x_0}{\hbar} \right) + \left(\frac{p_2^2 - p_1^2}{p_1 p_2} \right)^2 \sinh^2 \left(p_2 \frac{x_0}{\hbar} \right)} . \tag{5.6}$$

In the case of a tunnel diode, the barrier thickness is thin. It is possible to have $T \rightarrow 1$ in a limiting case of $x_0 = 0$. The transmitting wave is drawn in the lower part of Fig. 5.1 just to indicate that there is a definite probability of transmission even as $E - U_0 < 0$.

To calculate the tunneling of carriers from the valence band through the forbidden region due to the applied field as in the case of a tunnel diode, Zener¹ attempted to use Bloch's solution in a periodic field $U(x)$ perturbed by a uniform field \mathcal{E} . The resulting tunneling probability ζ is

$$\zeta = \frac{q\mathcal{E}a}{\hbar} \exp \left[-\frac{\pi}{4} \frac{(2m^*)^{1/2} E_g^{3/2}}{\hbar q\mathcal{E}} \right], \quad (5.7)$$

where \mathcal{E} is the applied field, a is the lattice constant, m^* is the effective mass of the carrier and E_g is the gap energy. The tunneling probability indicates that electrons are actually diffusing into regions where the kinetic energy is computed to be negative.

5.2 The Tunnel Diode. A tunnel diode is a p-n junction diode in which the p- and n-type regions have exceptionally large concentrations of acceptor and donor impurities. A tunnel diode exhibits two unusual regions in the V-I characteristic as shown in Fig. 5.2. At a very small forward bias, a region of negative resistance is observed. In the reverse bias region, the usual saturation region of the junction diode is absent. These characteristics will be explained in terms of the tunneling theory discussed in the above section.

1. Zener, C., "A Theory of the Electrical Breakdown of Solid Dielectrics", Proc. Roy. Soc., London, vol. A 145, p. 523; March, 1934.

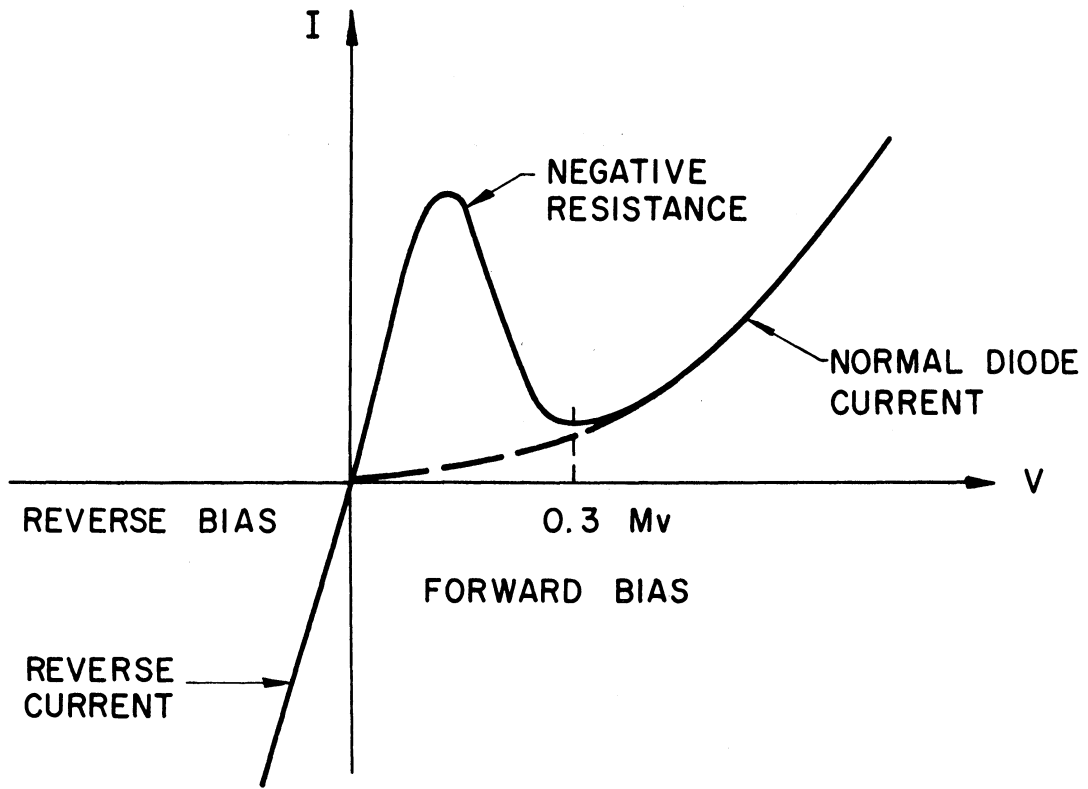
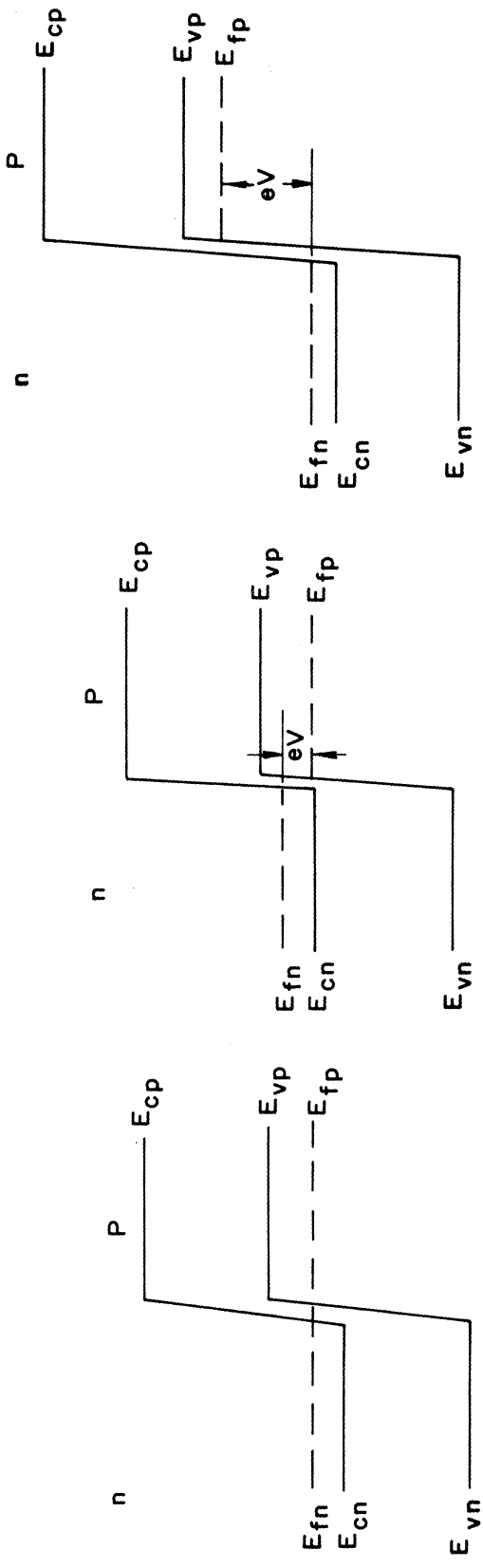


FIG. 5.2 THE V-I CHARACTERISTIC OF A TYPICAL TUNNEL DIODE.

The energy-level diagram of a tunnel diode is shown in Fig. 5.3. For a heavily doped semiconductor, the Fermi level for a p-type material is below the valence band energy and that for an n-type material is above the conduction band energy. When these materials are brought together into intimate contact, and when a small forward bias is applied, the electrons in the neighborhood of the Fermi-level in the conduction band of the n-type material are facing the holes in the neighborhood of the Fermi-level in the valence band of the p-type material directly across a forbidden gap. The tunneling probability is a maximum for the electrons in the n-type material to fall into the holes of the p-type material through the gap. This tunneling produces a negative resistance over a range of low forward bias. For a larger forward bias, tunneling ceases because there are no longer any conductor band states on the n-side at the same energy level as the valence band states on the p-side, and the current becomes the normal forward current observed in ordinary diodes.

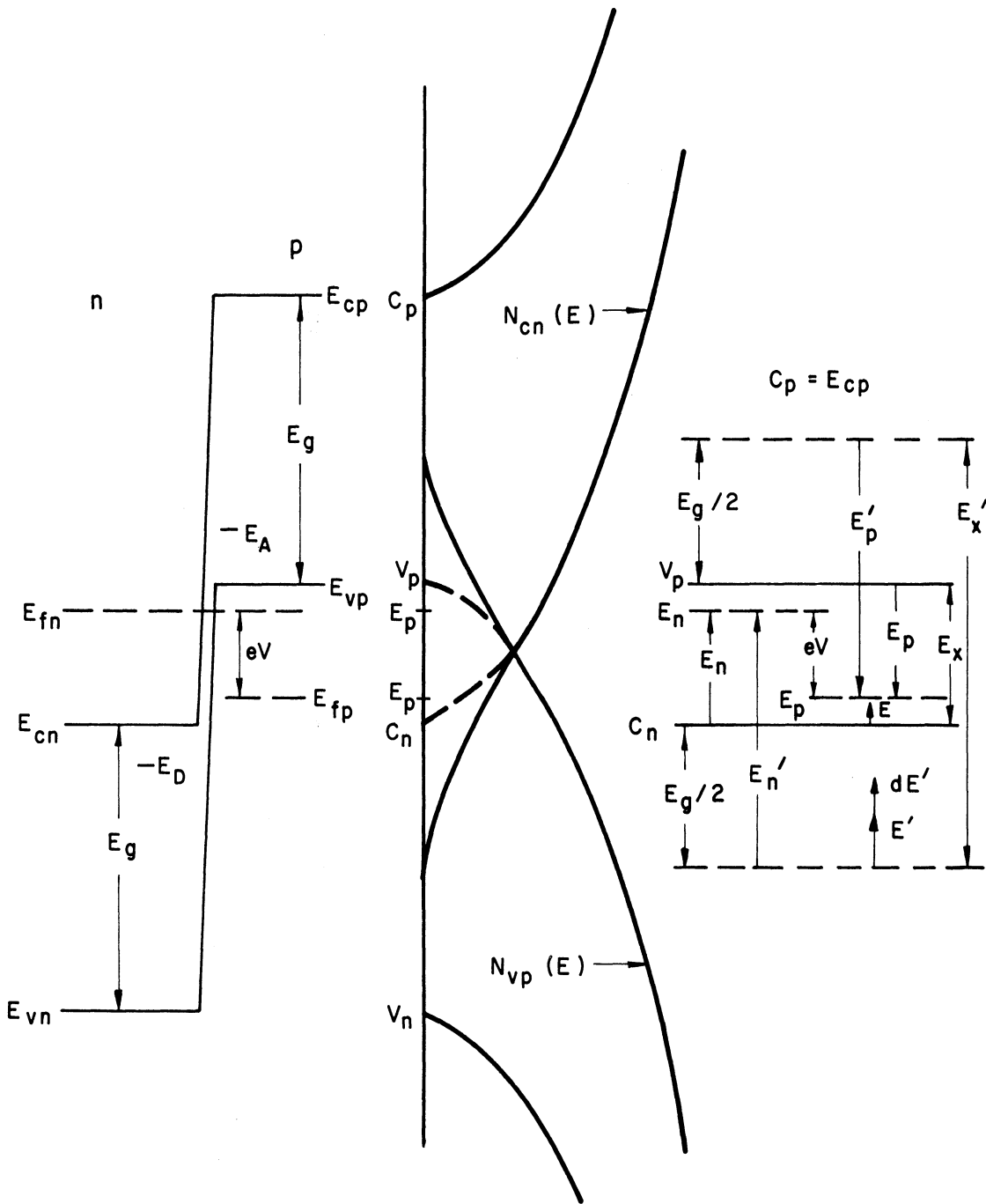
The behavior for reverse bias can also be predicted. In view of the energy level diagram in Fig. 5.3, tunneling also occurs when the Fermi-level on the p-side is higher than on the n-side. In fact, the higher the reverse voltage, the wider the range of levels that participate in tunneling and the larger the reverse current. Thus saturation under reverse bias will be absent.

5.3 The V-I Characteristic. Figure 5.4a shows an enlarged energy level diagram of a tunnel diode under the condition of a small forward bias similar to Fig. 5.3b. The forward bias voltage is V . E_{fp} and E_{fn} are the Fermi-level energies of the p- and n-type semiconductors



a.) ZERO BIAS, EQUILIBRIUM CONDITION b.) FORWARD BIAS c.) REVERSE BIAS

FIG. 5.3 ENERGY LEVEL DIAGRAM OF A TUNNEL DIODE.



a.) ENERGY LEVEL DIAGRAM OF A TUNNEL DIODE WITH FORWARD BIAS b.) DENSITY OF STATES IN A TUNNEL DIODE WITH FORWARD BIAS c.) RELATIVE POSITIONS OF THE ENERGY LEVELS

FIG. 5.4 ENERGY LEVEL DIAGRAM, DENSITY OF STATES AND THE DEFINITION OF TERMS USED IN ANALYZING THE V-I CHARACTERISTICS OF A TUNNEL DIODE.

respectively. If one defines the forward current as the tunneling current caused by electrons tunneling from the conduction band to the valence band, and the reverse current as the field emission current (or Zener current) caused by electrons passing from the valence band to the conduction band, then the total current at any time is the algebraic sum of these current, i.e.,

$$J = J_f + J_r .$$

The tunneling current density is proportional to the product of the density of occupied states on one side and the density of unoccupied states on the other side multiplied by the tunneling probability. Let $N_{cn}(E)$ and $N_{vp}(E)$ be the number of quantum states and $f_{cn}(E)$ and $f_{vp}(E)$ are the Fermi-Dirac probability functions of occupancy in the conduction and valence band of the n-type and p-type material respectively. Then $N_{cn}(E)f_{cn}(E)$ is the number of occupied quantum states of the energy E in the conduction band of the n-type material and $N_{vp}[1 - f_{vp}(E)]$ is the number of vacant quantum states of the same energy E in the valence band of the p-type material. Let $\zeta_{c \rightarrow v}$ be the probability of tunneling from c to v, then the forward tunneling current density J_f may be written as

$$J_f = \int_{E_{cn}}^{E_{vp}} N_{cn}(E) N_{vp}(E) \zeta_{c \rightarrow v}(E) f_{cn}(E) [1 - f_{vp}(E)] dE . \quad (5.8)$$

Notice that the integration is from E_{cn} to E_{vp} . This is because tunneling takes place only within this energy range.

Similarly, the tunneling current density in the reverse direction J_r can be expressed as

$$J_r = \int_{E_{vp}}^{E_{cn}} N_{cn}(E) N_{vp}(E) \zeta_{v \rightarrow c}(E) f_{vp}(E) [1 - f_{cn}(E)] dE \quad (5.9)$$

Thus the total tunneling current density becomes

$$J = \int_{E_{cn}}^{E_{vp}} N_{cn}(E) N_{vp}(E) \zeta_{c \rightarrow v} f_{cn}(E) [1 - f_{vp}(E)] dE - \int_{E_{cn}}^{E_{vp}} N_{cn}(E) N_{vp}(E) \zeta_{v \rightarrow c}(E) f_{vp}(E) [1 - f_{cn}(E)] dE \quad (5.10)$$

Assuming equal probability of tunneling from c to v as from v to c, the current density is written as

$$J = \int_{E_{cn}}^{E_{vp}} N_{cn}(E) N_{vp}(E) \zeta \left[f_{cn} (1 - f_{vp}(E)) - f_{vp}(E) (1 - f_{cn}(E)) \right] dE = \int_{E_{cn}}^{E_{vp}} N_{cn}(E) N_{vp}(E) \zeta \left[f_{cn}(E) - f_{vp}(E) \right] dE \quad (5.11)$$

The integral of Eq. 5.11 is extremely difficult to evaluate due to the following reasons:

1. The density of states is a complicated function of E. A tunnel diode consists of a simple p-n junction doped extra heavily with

impurities. Doping levels of more than 10^{19} atoms/cm³ are necessary to obtain significant tunneling. The heavy doping degenerates the semiconductor in which the Fermi-level will be located within the bands. In the n-type semiconductor, the Fermi-level is found in the conduction band, and in the p-type semiconductor it is found in the valence band. The high doping densities also cause the donor and acceptor impurity levels to be broadened into bands themselves and merge with the main bands. Figure 5.5 shows the density of states function for a degenerate n-type semiconductor. It can also be seen that band gap E_g narrows considerably to E'_g due to heavy doping. A similar sketch for the density of states function of a degenerate p-type semiconductor can also be drawn. The product of these two density of states functions is a highly irregular function of E and depends very much upon the doping concentrations.

2. The tunneling probability depends very much upon the potential barrier width and height and thus is a function of the junction field and the energy gap. It is further complicated by the fact that, although tunneling conditions require that energy and momentum be conserved, the conservation of momentum does not require the momentum of the electrons to be the same before and after the tunneling. This results in the two possible types of tunneling, the direct and indirect tunneling. In the direct tunneling, all particles participating in the tunneling must have the same energy on both sides of the barrier and they must tunnel from the vicinity of the minimum of the conduction band energy-momentum space to a corresponding energy-momentum space in the vicinity of the valence band. On the other hand, when the lowest conduction band minimum does

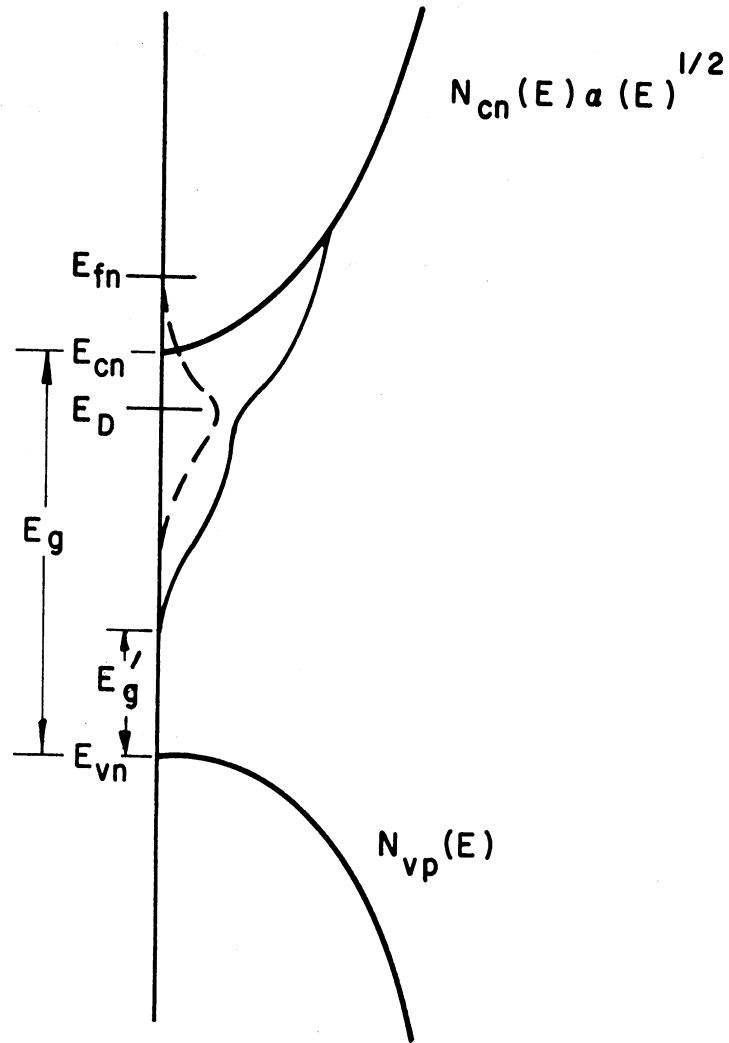


FIG. 5.5 THE DENSITY OF STATES FUNCTION FOR A DEGENERATE N-TYPE SEMICONDUCTOR SHOWING THE EFFECT OF BROADENING OF THE IMPURITY LEVEL E_D .

not occur at the same value of momentum space as the valence-band maximum, a condition which prevented the direct tunneling because of the violation of the law of conservation of momentum, indirect tunneling can exist. In this case, the difference in momentum is supplied by some scattering agents, such as phonons or impurities. It is thus very difficult to estimate the transition probability. Fortunately, the indirect-tunneling probability is generally considerably lower than the direct tunneling probability when direct tunneling is possible.

3. The Fermi-Dirac distribution function is temperature dependent. At absolute zero temperature, the Fermi-Dirac distribution function is a pure step function. At higher temperature the available states above the Fermi-level can be occupied with a nonzero probability.

All these factors introduce complications into the actual evaluation of Eq. 5.11. In fact, a general solution of Eq. 5.11 has not yet been found. Up to date, the only solution available is that for absolute zero temperature and in an assumed constant electric field configuration.

5.4 An Approximate Solution of the V-I Characteristic. To facilitate the solution of the integral of Eq. 5.11, it is desirable to investigate each term of the integral carefully. The density of states terms, $N_{cn}(E)$ and $N_{vp}(E)$, will be discussed first. Figure 5.4b is a sketch of the density of states graph of a tunnel diode with a forward bias. On the left-hand side of this figure, Fig. 5.4a, the energy level diagram of the tunnel diode under the above stated operating condition is reproduced for clarity. A slight change in notation is in effect in order to simplify the subscripts. For example E_{cp} , the conductor level on p-side, is abbreviated as C_p , E_{vp} as V_p , etc. On

the right-hand side of the graph, shown as Fig. 5.4c, notations and reference of the energy levels are indicated.

In Fig. 5.4b, $N_{cn}(E)$ and $N_{vp}(E)$ are drawn as solid curves. These are the modified density of states curves in which the effect of the broadening of the donor or acceptor band are taken into account. If there were no broadening effect of the impurity levels, these curves would follow the dotted extensions of the curves. In fact, the broadening effect of the impurity level is the result of heavy doping. Although the detailed calculation of the broadening effect is complicated, one could make a rough estimate by assuming that $N_{cn}(E)$ would start from an energy level E'_g somewhere in the band gap and increase gradually toward the original $N_{cn}(E)$ at V_p . Similarly, $N_{vp}(E)$ is also shown. Let us assume that for equal impurity concentration on both sides, E'_g is approximately halfway between the band gap and that

$$N_{cn}(E) = A_1(E')^{4/3^*}$$

and

$$N_{vp}(E) = A_2(E'_x - E')^{4/3} \quad , \quad (5.12)$$

where the relative positions of E' and E'_x with respect to other levels in shown in Fig. 5.4c, and

$$\begin{aligned} E' &= E + E_g/2 \quad , \\ E'_x &= E_x + E_g \quad , \end{aligned} \quad (5.13)$$

* The choice of $4/3$ power is arbitrary. It is determined from the best available experimental data on broadening by heavy doping.

E being the energy level with respect to C_n (or zero). Notice that without the broadening effect, $N_{cn}(E) = A E^{1/2}$ and $N_{vp}(E) = A(E_x - E)^{1/2}$.

The Fermi-factors are defined as

$$f_{cn}(E) = \frac{1}{1 + e^{(E' - E'_n)/kT}} \quad , \quad (5.14a)$$

$$f_{vp}(E) = \frac{1}{1 + e^{[E' - (E'_x - E'_p)]/kT}} \quad (5.14b)$$

and

$$f_{cn}(E) - f_{vp}(E) = \frac{2 \left(\frac{eV}{2kT} \right)}{\sinh \frac{eV}{2kT} + \cosh \frac{eV + 2(E' - E'_n)}{2kT}} \quad , \quad (5.15)$$

where

$$eV = E'_n - E'_p = E_n - E_p \quad .$$

Define

$$E'_x \triangleq E_g + E_n + E_p - eV \quad (5.16)$$

and

$$x \triangleq (2 E'/E'_x) - 1 \quad (5.17)$$

and assuming for each impurity concentration,

$$E'_n = E'_p = eV_m/2 \quad , \quad (5.18)$$

then

$$\frac{eV + 2(E' - E'_n)}{2kT} = \frac{1}{2} \frac{e}{kT} (V_m - V) x .$$

Equation 5.15 can be modified as

$$f_{cn}(E) - f_{vp}(E) = \frac{\sinh\left(\frac{eV}{2kT}\right)}{\cosh\frac{eV}{2kT} + \cosh\frac{1}{2} \cdot \frac{e}{kT} (V_m - V) x} . \quad (5.19)$$

Assume also for the time being that the transition probability between n and p are equal and 100 percent, then Eq. 5.11 can be expressed in terms of x as

$$\begin{aligned} J &= A^2 \left(\frac{e(V_m - V)}{2}\right)^{5/3} \sinh\left(\frac{eV}{2kT}\right) \int_{-1}^1 \frac{(1-x^2)^{4/3} dx}{\cosh\left(\frac{eV}{2kT}\right) + \cosh\frac{e}{2kT} (V_m - V)x} \\ &= B^2 \left(\frac{1}{kT}\right)^2 \left[\frac{e(V_m - V)}{2}\right]^{5/3} \sinh\left(\frac{eV}{2kT}\right) \int_{-1}^1 \frac{(1-x^2)^{4/3} dx}{\cosh\left(\frac{eV}{2kT}\right) + \cosh\frac{e}{2kT} (V_m - V)x} , \end{aligned} \quad (5.20)$$

where B is a constant.

Equation 5.20 is useful in predicting the effect of several factors on the tunneling current density. The doping concentration will appear in the choice of V_m , the temperature effect in T and the bias effect in V.

5.5 Future Work. Equation 5.20 will be evaluated under various prescribed operating conditions, particularly when the forward bias is

varied. For a particular sample of semiconductor material, and at a particular operating temperature, the variation of V , the forward or reverse bias voltage should result in a V - I characteristic which can be checked experimentally.

When the tunnel diode is used as an amplifier, the negative resistance portion of the V - I characteristic is of importance. To compute the cross-modulation products due to the nonlinear portion of the characteristic, Eq. 5.20 or its modification will be used for multiple-signal operation. It is planned that series development of the terms involved in this equation will be used for this analysis.

The effect of tunneling probability ξ can also be included if an adequate approximation can be found.

6. Nonlinear Analysis of the Crossed-Field Amplifier with Multi-Signal Input (M. E. El-Shandwily, J. E. Rowe)

6.1 Introduction. During the previous period a study of the nonlinear operation of the injected-beam forward-wave crossed-field amplifier with multi-signal input was initiated. A small-signal nonlinear analysis has been completed during this period. A brief discussion of the analysis is given in the following section.

6.2 Theoretical Analysis. It is assumed that at the tube input the voltage applied consists of N -signals which can be written as

$$V_{in} = \operatorname{Re} \sum_{n=1}^N V_n e^{j\omega_n t}, \quad (6.1)$$

where the frequencies $\omega_1, \dots, \omega_N$ are within the bandwidth of the tube. Due to the nonlinearity of the beam-circuit interaction the output

spectrum will contain frequency components which are not present in the input. It is the purpose of this analysis to derive expressions for the different frequency components in the output.

The starting point is to neglect the nonlinearity and consider the circuit voltage as a superposition of the effect of the individual input signals according to the linear theory. This circuit voltage is then assumed to act on the electrons whose motion can be calculated by successive approximations. It will therefore be possible to express the longitudinal and transverse coordinates of the electrons as a power series of the input voltages. From these relations one can calculate the arrival time of the electrons at some longitudinal distance in terms of their departure time at the input plane and therefore the r-f charge in the beam. The induced voltage in the circuit is due to two effects, the first is the r-f charge whose effect is similar to the O-type case, the second is the r-f displacement which in the presence of a longitudinal field that varies with the transverse position will produce a circuit voltage even if the density of the beam does not vary along the direction of propagation.

The induced voltage on the circuit is given by

$$V = \frac{-j \omega \Gamma_o K}{\Gamma^2 - \Gamma_o^2} \rho_E , \quad (6.2)$$

where Γ_o , Γ are the propagation constants of the circuit in the absence and presence of the beam respectively, K is the circuit impedance and ρ_E is the effective charge density of the beam at the frequency ω .

The effective charge density, ρ_E , can be written as

$$\rho_E = (\rho_0 + \rho) \varphi(y) , \quad (6.3)$$

where ρ_0 is the d-c charge density, ρ is the r-f charge density and $\varphi(y)$ is the coupling function. The coupling function will be expanded in a Taylor series about the unperturbed position of the beam

$$\begin{aligned} \varphi(y) = \varphi(y_0) + \frac{d\varphi}{dy}\Big|_{y_0} (y - y_0) + \frac{1}{2!} \frac{d^2\varphi}{dy^2}\Big|_{y_0} (y - y_0)^2 \\ + \frac{1}{3!} \frac{d^3\varphi}{dy^3}\Big|_{y_0} (y - y_0)^3 + \dots , \quad (6.4) \end{aligned}$$

therefore the effective r-f charge density can be written as

$$\begin{aligned} \rho_E = \rho\varphi(y_0) + \rho_0(y-y_0) \frac{d\varphi}{dy}\Big|_{y_0} + \rho(y-y_0) \frac{d\varphi}{dy}\Big|_{y_0} + \frac{1}{2!} \rho_0 (y-y_0)^2 \frac{d^2\varphi}{dy^2}\Big|_{y_0} \\ + \frac{1}{2!} \rho (y-y_0)^2 \frac{d^2\varphi}{dy^2}\Big|_{y_0} + \frac{1}{3!} \rho_0 (y-y_0)^3 \frac{d^3\varphi}{dy^3}\Big|_{y_0} + \dots . \quad (6.5) \end{aligned}$$

The first term, $\rho\varphi(y_0)$, gives the effective charge density due to the longitudinal r-f charge at the unperturbed beam position. The terms $\rho_0 (y-y_0) (d\varphi/dy)|_{y_0}$, $(1/2) \rho_0 (y-y_0)^2 (d^2\varphi/dy^2)|_{y_0}$ and $(1/3) \rho_0 (y-y_0)^3 (d^3\varphi/dy^3)|_{y_0}$ give the effective charge due to the r-f transverse displacement of the d-c charge of the beam. The remaining two terms, namely $\rho(y-y_0) (d\varphi/dy)|_{y_0}$ and $(1/2) \rho (y-y_0)^2 (d^2\varphi/dy^2)|_{y_0}$, give the effective charge due to r-f displacement of the r-f charge density. It should be noted that since ρ_E is a real quantity then

when ρ and $y-y_0$ are expressed in a complex form the real part has to be taken first and then the multiplication is performed.

As has been mentioned previously, the equations of motion and the successive approximations described above are used to obtain expressions for the r-f charge density, ρ , and the r-f transverse displacement, $(y-y_0)$. There will be an expression for each frequency component of the charge density. The r-f transverse displacement $(y-y_0)$ which is obtained from the equations of motion will have components at all possible frequency combinations. Since in this analysis the perturbation is carried only to the third order, that is, the y and z displacements are obtained in terms of the input voltages, their squares and cubes, then only the components with the following frequencies will be found both in ρ and $(y-y_0)$ f_r , $f_r \pm f_p$, $2f_r - f_p$ and $f_r + f_p - f_s$, where r, p, or s = 1, 2, ..., N. To obtain the effective charge density at a particular frequency care must be taken to include all the contributions of the different terms in Eq. 6.5. For example the r-f charge density at $f_r \pm f_p$ will contribute an effective charge density at $f_r \pm f_p \pm f_s$ when multiplied by the appropriate part of $(y-y_0)$ in the third term of Eq. 6.5. Physically, this is because an r-f charge density at $f_r \pm f_p$ will have an r-f transverse displacement at f_s and therefore it produces a circuit voltage at the combined frequency $f_r \pm f_p \pm f_s$.

To simplify the analysis the following assumptions are made:

1. The beam is assumed to be very thin so that the difference between the fields on both sides of the beam is neglected.
2. Space-charge forces are neglected.
3. Only the increasing wave of each input signal is considered.
4. The adiabatic equations of motion are used.

In addition to the above assumptions the usual assumptions which are commonly used in the analysis of such devices are also utilized, namely nonrelativistic mechanics, no thermal velocity distribution and no reflections.

According to these assumptions the equations of motion of any electron that entered the interaction space at time t_0 are written as:

$$\frac{dz}{d\tau} = \frac{|\eta|}{\omega_c} \operatorname{Re} \sum_{n=1}^N \left\{ V'_n \left[\frac{d\varphi_n}{dy} \Big|_{y_0} + \frac{d^2\varphi_n}{dy^2} \Big|_{y_0} (y-y_0) + \frac{1}{2} \frac{d^3\varphi_n}{dy^3} \Big|_{y_0} (y-y_0)^2 \right] e^{-\Gamma_n z} e^{j\omega_n \tau + j\omega_n t_0} \right\} \quad (6.6)$$

and

$$\frac{dy}{d\tau} = \frac{|\eta|}{\omega_c} \operatorname{Re} \sum_{n=1}^N \left\{ V'_n \Gamma_n \left[\varphi_n(y_0) + \frac{d\varphi_n}{dy} \Big|_{y_0} (y-y_0) + \frac{1}{2!} \frac{d^2\varphi_n}{dy^2} \Big|_{y_0} (y-y_0)^2 + \frac{1}{3!} \frac{d^3\varphi_n}{dy^3} \Big|_{y_0} (y-y_0)^3 \right] e^{-\Gamma_n z} e^{j\omega_n \tau + j\omega_n t_0} \right\}, \quad (6.7)$$

where η is the electron charge-to-mass ratio,

ω_c is the cyclotron radian frequency,

V'_n is the amplitude of the increasing wave of the nth signal at the input plane $z = 0$,

$\Gamma_n = j\beta_{en}(1 + jD_n \delta_n)$ is the propagation constant of the increasing wave of the nth signal,

$\beta_{en} = \omega_n / u_0$,

D_n is the interaction parameter,

$\tau = t - t_0$ is the transit time,

t_0 is the entrance time and

Re denotes the real part.

The first approximation to solve Eqs. 6.6 and 6.7 is to substitute $y = y_0$ and $z = u_0 \tau$ on the right-hand side of Eqs. 6.6 and 6.7 and integrate with respect to τ . The result is

$$z = u_0 \tau + \frac{1}{2\beta_c V_0} \sum_{n=1}^N \Omega_n \frac{V_n'}{D_n} X_n^{(1)} e^{\xi_n \gamma_n \tau} \cos (\omega_n t_0 - \theta_n^{(1)} + \xi_n \alpha_n \tau) \quad (6.8)$$

and

$$y = y_0 + \frac{1}{2\beta_c V_0} \sum_{n=1}^N \psi_n \frac{V_n'}{D_n} X_n^{(1)} e^{\xi_n \gamma_n \tau} \cos (\omega_n t_0 - \theta_n^{(1)} + \xi_n \alpha_n \tau) , \quad (6.9)$$

where $X_n^{(1)} e^{-j\theta_n^{(1)}} = 1/\delta_n$,

$$\xi_n = \beta_{en} D_n u_0,$$

$$\delta_n = \gamma_n + j\alpha_n,$$

$$\beta_c = \omega_c / u_0,$$

$$\Omega_n = \cosh \beta_{en} y_0 / \sinh \beta_{en} d \text{ and}$$

$$\psi_n = \sinh \beta_{en} y_0 / \sinh \beta_{en} d.$$

In writing the above equations it has been assumed that $\phi_n(y) = \sinh \beta_{en} y / \sinh \beta_{en} d$ and the anode-sole spacing is d . The second approximation is obtained by substituting from Eqs. 6.8 and 6.9 into the right-hand side of Eqs. 6.6 and 6.7 and neglecting the second-order

terms of $(y-y_0)$. Also the factor $e^{-\Gamma_n z}$ in both Eqs. 6.6 and 6.7 will be written as

$$e^{-\Gamma_n u_0 \tau} \left[1 - \frac{\Gamma_n}{2\beta_c v_0} \sum_{i=1}^N \frac{\Omega_i}{D_i} V_i' X_i^{(1)} e^{\xi_i \gamma_i \tau} \cos (\omega_i t_0 - \theta_i^{(1)} + \xi_i \gamma_i \tau) \right]$$

and then the integration is performed with respect to τ . The process is repeated to obtain the third-order approximation. The result of these steps is an expression for z and y in terms of the input voltages, their squares and their cubes and the departure and transit times.

The continuity equation of the charge density is used to obtain expressions for the r-f current (or charge density) at the various frequencies as it has been done in the O-type amplifier. After going through extremely complicated algebra the following components of the output voltage are derived:

$$\begin{aligned}
 \frac{V_{f_r}}{V_{inr}} &= \left(\frac{V'_r}{V_{inr}} \right) \frac{1 + D_r b_r - jD_r d_r}{\delta_r (\delta_r + j b_r + d_r)} e^{\zeta_r \delta_r} \\
 &+ 4 \left(\frac{P_{inr}}{I_o V_o} \right) \left(\frac{V'_r}{V_{inr}} \right)^3 \frac{(1 + D_r b_r - jD_r d_r)}{\{j(\delta_r + 2\gamma_r) - b_r + jd_r\}} \left(\frac{\Omega_r}{\Psi_r} \right) e^{\zeta_r (\delta_r + 2\gamma_r)} \\
 &\cdot \left[jG + \frac{\Omega_r}{\Psi_r} H + \frac{1}{2} L + \frac{1}{3} \frac{\Omega_r}{\Psi_r} M \right] \\
 &+ 4 \sum_{\substack{i=1 \\ i \neq r}}^N \left\{ \left(\frac{P_{ini}}{I_o V_o} \right) \left(\frac{V'_i}{V_{ini}} \right)^2 \left(\frac{V'_r}{V_{inr}} \right) \left(\frac{\Omega_r}{\Omega_i} \right) \right. \\
 &\cdot \left(\frac{\Omega_r}{\Psi_i} \right) \frac{1 + D_r b_r - jD_r d_r}{\left\{ j \left(\delta_r + 2 \frac{D_i}{D_r} \frac{\beta_i}{\beta_r} \gamma_i \right) - b_r + jd_r \right\}} e^{\zeta_r \delta_r + 2\zeta_i \gamma_i} \\
 &\left. \cdot \left[jQ + \frac{\Omega_r}{\Psi_r} P + \frac{1}{2} S + \frac{1}{3} \frac{\Omega_r}{\Psi_r} T \right] \right\}, \quad (6.10)
 \end{aligned}$$

where

$$\begin{aligned}
 G = & \frac{\beta_r}{\beta_c} \frac{1}{16} \left[-\frac{1}{4} X_r^{(1)} X_r^{(1)} X_r^{(1)} e^{-j\theta_r^{(1)}} + j X_r^{(1)} X_r^{(1)} X_{rr}^{(3)} e^{-j\theta_r^{(1)}} \right. \\
 & \cdot \left\{ \left(\frac{\psi_r}{\Omega_r} \right)^2 \cos (\theta_r^{(1)} - \theta_{rr}^{(3)}) + \sin (\theta_r^{(1)} - \theta_{rr}^{(3)}) \right\} \\
 & + \frac{j}{2} X_r^{(1)} X_r^{(1)} X_{rr}^{(2)} e^{-j\theta_{rr}^{(2)}} \left\{ -j + \left(\frac{\psi_r}{\Omega_r} \right)^2 \right\} \\
 & + X_r^{(1)} X_{rr}^{(3)} X_{rrr}^{(6)} e^{-j\theta_{rrr}^{(6)}} \left\{ (1-j) \left(\frac{\psi_r}{\Omega_r} \right)^2 \cos (\theta_r^{(1)} - \theta_{rr}^{(3)}) \right. \\
 & \left. - \left(j + \left(\frac{\psi_r}{\Omega_r} \right)^2 \right) \sin (\theta_r^{(1)} - \theta_{rr}^{(3)}) \right\} + \left(\frac{\psi_r}{\Omega_r} \right)^2 X_r^{(1)} X_r^{(1)} X_{rrr}^{(6)} e^{-j\theta_{rrr}^{(6)}} (1-j) \\
 & + \frac{1}{2} X_r^{(1)} X_{rr}^{(2)} X_{rrr}^{(5)} e^{-j(\theta_r^{(1)} + \theta_{rr}^{(2)} - \theta_{rrr}^{(5)})} \left\{ 1 + \left(\frac{\psi_r}{\Omega_r} \right)^2 (1+2j) \right\} \\
 & \left. + \frac{1}{2} \left(\frac{\psi_r}{\Omega_r} \right)^2 X_r^{(1)} X_r^{(1)} X_{rrr}^{(5)} e^{-j(2\theta_r^{(1)} - \theta_{rrr}^{(5)})} (1+j) \right] ,
 \end{aligned}$$

$$\begin{aligned}
 H = & \frac{\beta_r}{\beta_c} \frac{1}{16} \left[X_r^{(1)} X_{rr}^{(3)} X_{rrr}^{(5)} e^{-j\theta_{rrr}^{(5)}} \frac{\psi_r}{\Omega_r} \left\{ \left(j + \left(\frac{\psi_r}{\Omega_r} \right)^2 \right) \cos (\theta_r^{(1)} - \theta_{rr}^{(3)}) \right. \right. \\
 & + (1 - j) \sin (\theta_r^{(1)} - \theta_{rr}^{(3)}) \left. \left. \right\} + \frac{\psi_r}{\Omega_r} X_r^{(1)} X_r^{(1)} X_{rrr}^{(5)} e^{-j\theta_{rr}^{(5)}} \left\{ 1 + \frac{j}{2} \left(\frac{\psi_r}{\Omega_r} \right)^2 \right\} \right. \\
 & + \frac{\psi_r}{\Omega_r} X_r^{(1)} X_r^{(2)} X_{rrr}^{(5)} e^{-j(\theta_r^{(1)} + \theta_{rr}^{(2)} - \theta_{rrr}^{(5)})} \left\{ -j + \frac{1}{2} + \frac{1}{2} \left(\frac{\psi_r}{\Omega_r} \right)^2 \right\} \\
 & + \frac{1}{2} \frac{\psi_r}{\Omega_r} X_r^{(1)} X_r^{(1)} X_{rrr}^{(5)} e^{-j(2\theta_r^{(1)} - \theta_{rrr}^{(5)})} \left\{ 1 - \frac{j}{2} \left(\frac{\psi_r}{\Omega_r} \right)^2 \right\} \\
 & + j \frac{\psi_r}{\Omega_r} X_r^{(1)} X_r^{(1)} X_{rr}^{(3)} e^{-j\theta_r^{(1)}} \left\{ \cos (\theta_r^{(1)} - \theta_{rr}^{(3)}) - \sin (\theta_r^{(1)} - \theta_{rr}^{(3)}) \right\} \\
 & - \frac{\psi_r}{\Omega_r} X_r^{(1)} X_r^{(1)} X_r^{(1)} e^{-j\theta_r^{(1)}} \\
 & \left. + \frac{\psi_r}{\Omega_r} X_r^{(1)} X_r^{(1)} X_{rr}^{(2)} e^{-j\theta_{rr}^{(2)}} \left\{ \frac{3}{2} - \frac{j}{2} + j \left(\frac{\psi_r}{\Omega_r} \right)^2 \right\} \right] ,
 \end{aligned}$$

$$L = \frac{\beta_r}{\beta_c} \frac{1}{16} \left[2 \left(\frac{\psi_r}{\Omega_r} \right)^2 X_r^{(1)} X_r^{(1)} X_{rr}^{(3)} e^{-j\theta_r^{(1)}} \right. \\ \cdot \left\{ \cos (\theta_r^{(1)} - \theta_{rr}^{(3)}) - \sin (\theta_r^{(1)} - \theta_{rr}^{(3)}) \right\} \\ + \left(\frac{\psi_r}{\Omega_r} \right)^2 X_r^{(1)} X_r^{(1)} X_{rr}^{(2)} e^{-j\theta_{rr}^{(2)}} (1 + j) \\ \left. + \frac{j}{2} \left(\frac{\psi_r}{\Omega_r} \right)^2 X_r^{(1)} X_r^{(1)} X_r^{(1)} e^{-j\theta_r^{(1)}} \right],$$

$$M = \frac{3}{32} \frac{\beta_r}{\beta_c} \left(\frac{\psi_r}{\Omega_r} \right)^3 X_r^{(1)} X_r^{(1)} X_r^{(1)} e^{-j\theta_r^{(1)}},$$

$$Q = \frac{1}{16} \left[-\frac{1}{2} \frac{\beta_r}{\beta_c} \frac{\beta_r}{\beta_i} \left(\frac{\Omega_i}{\Omega_r} \right)^2 X_r^{(1)} X_i^{(1)} X_i^{(1)} e^{-j\theta_r^{(1)}} \right. \\ + j \frac{\beta_r}{\beta_c} X_r^{(1)} X_i^{(1)} X_{ii}^{(3)} e^{-j\theta_r^{(1)}} \left\{ \left(\frac{\psi_i}{\Omega_r} \right)^2 \cos (\theta_i^{(1)} - \theta_{ii}^{(3)}) \right. \\ \left. + \left(\frac{\Omega_i}{\Omega_r} \right)^2 \sin (\theta_i^{(1)} - \theta_{ii}^{(3)}) \right\} + \frac{j}{2} \frac{\beta_r}{\beta_c} \frac{\Omega_i}{\Omega_r} X_i^{(1)} e^{-j\theta_i^{(1)}} \\ \cdot \left\{ \frac{\beta_r}{\beta_i} X_i^{(1)} X_{ri}^{(3)} e^{j(\theta_i^{(1)} - \theta_{ri}^{(3)})} \left(\frac{\psi_i}{\Omega_r} \frac{\psi_r}{\Omega_r} - j \frac{\Omega_i}{\Omega_r} \right) \right. \\ \left. + X_r^{(1)} X_{ir}^{(3)} e^{-j(\theta_r^{(1)} - \theta_{ir}^{(3)})} \left(\frac{\psi_i}{\Omega_r} \frac{\psi_r}{\Omega_r} + j \frac{\Omega_i}{\Omega_r} \right) \right\} \right]$$

(Q Contd.)

$$\begin{aligned}
 & + \frac{j}{2} \frac{\beta_r}{\beta_c} \frac{\Omega_i}{\Omega_r} \left(\frac{\psi_i}{\Omega_r} \frac{\psi_r}{\Omega_r} - j \frac{\Omega_i}{\Omega_r} \right) \left\{ \frac{\beta_r}{\beta_i} X_i^{(1)} X_i^{(1)} X_{ri}^{(2)} e^{-j\theta_{ri}^{(2)}} \right. \\
 & + X_i^{(1)} X_r^{(1)} X_{ir}^{(2)} e^{j(\theta_i^{(1)} - \theta_r^{(1)} - \theta_{ir}^{(2)})} \left. \right\} + \frac{\beta_r}{\beta_c} X_i^{(1)} X_{ii}^{(3)} X_{rii}^{(6)} e^{-j\theta_{rii}^{(6)}} \\
 & \cdot \left\{ \left(\frac{\Omega_i}{\Omega_r} \frac{\psi_r}{\Omega_r} \frac{\psi_i}{\Omega_r} - j \left(\frac{\psi_i}{\Omega_r} \right)^2 \right) \cos (\theta_i^{(1)} - \theta_{ii}^{(3)}) \right. \\
 & - \left. \left(\frac{\Omega_i}{\Omega_r} \frac{\psi_r}{\Omega_r} \frac{\psi_i}{\Omega_r} + j \left(\frac{\psi_i}{\Omega_r} \right)^2 \right) \sin (\theta_i^{(1)} - \theta_{ii}^{(3)}) \right\} \\
 & + \frac{1}{2} \frac{\psi_i}{\Omega_r} X_{iri}^{(6)} e^{-j\theta_{iri}^{(6)}} \left\{ \frac{\beta_r}{\beta_c} \left(\frac{\Omega_i}{\Omega_r} \frac{\psi_r}{\Omega_r} + j \frac{\psi_i}{\Omega_r} \right) X_i^{(1)} X_{ri}^{(3)} e^{j(\theta_i^{(1)} - \theta_{ri}^{(3)})} \right. \\
 & + \frac{\beta_i}{\beta_c} \left(\frac{\psi_i}{\Omega_r} - j \frac{\Omega_i}{\Omega_r} \frac{\psi_r}{\Omega_r} \right) X_r^{(1)} X_{ir}^{(3)} e^{-j(\theta_r^{(1)} - \theta_{ir}^{(3)})} \left. \right\} \\
 & - \frac{j}{2} \frac{\Omega_i}{\Omega_r} X_{iri}^{(6)} e^{-j\theta_{iri}^{(6)}} \left\{ \frac{\beta_r}{\beta_c} \left(\frac{\psi_i}{\Omega_r} \frac{\psi_r}{\Omega_r} - j \frac{\Omega_i}{\Omega_r} \right) X_i^{(1)} X_{ri}^{(3)} e^{j(\theta_i^{(1)} - \theta_{ri}^{(3)})} \right. \\
 & + \frac{\beta_i}{\beta_c} \left(\frac{\psi_i}{\Omega_r} \frac{\psi_r}{\Omega_r} + j \frac{\Omega_i}{\Omega_r} \right) X_r^{(1)} X_{ir}^{(3)} e^{-j(\theta_r^{(1)} - \theta_{ir}^{(3)})} \left. \right\} \\
 & + \frac{\beta_i}{\beta_c} \frac{\psi_i}{\Omega_r} X_i^{(1)} X_r^{(1)} X_{iri}^{(6)} e^{j(\theta_i^{(1)} - \theta_r^{(1)} - \theta_{iri}^{(6)})} \left\{ \frac{\psi_r}{\Omega_r} \frac{\Omega_i}{\Omega_r} - \frac{j}{2} \left(\frac{\psi_i}{\Omega_r} + \frac{\psi_r}{\Omega_r} \frac{\Omega_i}{\Omega_r} \right) \right\} \\
 & + \frac{\beta_r}{\beta_i} \frac{\beta_r}{\beta_c} \frac{\psi_i}{\Omega_r} X_i^{(1)} X_i^{(1)} X_{rii}^{(6)} e^{-j\theta_{rii}^{(6)}} \left\{ \frac{\psi_i}{\Omega_r} - j \frac{\psi_r}{\Omega_r} \frac{\Omega_i}{\Omega_r} \right\}
 \end{aligned}$$

(Q Contd.)

$$+ \frac{1}{2} \frac{\beta_i}{\beta_c} X_r^{(1)} X_{ir}^{(2)} X_{iir}^{(5)} e^{-j(\theta_r^{(1)} + \theta_{ir}^{(2)} - \theta_{iir}^{(5)})}$$

$$\cdot \left\{ \left(\frac{\psi_i}{\Omega_r} \right)^2 + 2j \frac{\psi_i}{\Omega_r} \frac{\psi_r}{\Omega_r} \frac{\Omega_i}{\Omega_r} + \left(\frac{\Omega_i}{\Omega_r} \right)^2 \right\}$$

$$+ \frac{1}{2} \frac{\beta_r}{\beta_c} X_i^{(1)} X_{ri}^{(2)} X_{iir}^{(5)} e^{-j(\theta_i^{(1)} + \theta_{ri}^{(2)} - \theta_{iir}^{(5)})}$$

$$\cdot \left\{ \frac{\psi_i}{\Omega_r} \frac{\psi_r}{\Omega_r} \frac{\Omega_i}{\Omega_r} + j \left(\frac{\psi_i}{\Omega_r} \right)^2 + \left(\frac{\Omega_i}{\Omega_r} \right)^2 + j \frac{\psi_i}{\Omega_r} \frac{\psi_r}{\Omega_r} \frac{\Omega_i}{\Omega_r} \right\}$$

$$+ \frac{\beta_i}{\beta_c} \frac{\psi_i}{\Omega_r} X_i^{(1)} X_r^{(1)} X_{iir}^{(5)} e^{-j(\theta_i^{(1)} + \theta_r^{(1)} - \theta_{iir}^{(5)})}$$

$$\left\{ \frac{\Omega_i}{\Omega_r} \frac{\psi_r}{\Omega_r} + \frac{j}{2} \frac{\Omega_i}{\Omega_r} \frac{\psi_r}{\Omega_r} + \frac{j}{2} \frac{\psi_i}{\Omega_r} \right\} \Bigg] ,$$

$$P = \frac{1}{16} \left[\frac{\beta_r}{\beta_c} X_i^{(1)} X_{ii}^{(3)} X_{rii}^{(6)} e^{-j\theta_{rii}^{(6)}} \left\{ \frac{\psi_i}{\Omega_r} \left(j \frac{\Omega_i}{\Omega_r} + \frac{\psi_i}{\Omega_r} \frac{\psi_r}{\Omega_r} \right) \cos (\theta_i^{(1)} - \theta_{ii}^{(3)}) \right. \right.$$

$$\left. + \frac{\Omega_i}{\Omega_r} \left(-j \frac{\psi_i}{\Omega_r} + \frac{\Omega_i}{\Omega_r} \frac{\psi_r}{\Omega_r} \right) \sin (\theta_i^{(1)} - \theta_{ii}^{(3)}) \right\}$$

$$+ \frac{1}{2} \frac{\beta_r}{\beta_c} X_i^{(1)} X_{ri}^{(3)} X_{iri}^{(6)} e^{j(\theta_i^{(1)} - \theta_{ri}^{(3)} - \theta_{iri}^{(6)})}$$

$$\cdot \left\{ j \left(\frac{\Omega_i}{\Omega_r} \right)^2 \frac{\psi_r}{\Omega_r} - \frac{\Omega_i}{\Omega_r} \frac{\psi_i}{\Omega_r} - j \frac{\psi_i}{\Omega_r} \frac{\Omega_i}{\Omega_r} + \left(\frac{\psi_i}{\Omega_r} \right)^2 \frac{\psi_r}{\Omega_r} \right\}$$

(P Contd.)

$$\begin{aligned}
 & + \frac{1}{2} \frac{\beta_i}{\beta_c} X_r^{(1)} X_{ir}^{(3)} X_{iri}^{(6)} e^{j(-\theta_r^{(1)} + \theta_{ir}^{(3)} - \theta_{iri}^{(6)})} \\
 & \cdot \left\{ j \left(\frac{\Omega_i}{\Omega_r} \right) \frac{\psi_i}{\Omega_r} + \left(\frac{\Omega_i}{\Omega_r} \right)^2 \frac{\psi_r}{\Omega_r} + j \frac{\psi_i}{\Omega_r} \frac{\Omega_i}{\Omega_r} + \left(\frac{\psi_i}{\Omega_r} \right)^2 \frac{\psi_r}{\Omega_r} \right\} \\
 & + \frac{\beta_r}{\beta_c} \frac{\beta_r}{\beta_i} \frac{\psi_i}{\Omega_r} X_i^{(1)} X_i^{(1)} X_{rii}^{(6)} e^{-j\theta_{rii}^{(6)}} \left\{ \frac{j}{2} \frac{\psi_i}{\Omega_r} \frac{\psi_r}{\Omega_r} + \frac{\Omega_i}{\Omega_r} \right\} \\
 & + \frac{1}{2} \frac{\beta_i}{\beta_c} X_r^{(1)} X_i^{(1)} X_{iri}^{(6)} e^{j(\theta_i^{(1)} - \theta_r^{(1)} - \theta_{iri}^{(6)})} \\
 & \cdot \left\{ j \left(\frac{\psi_i}{\Omega_r} \right)^2 \frac{\psi_r}{\Omega_r} + \frac{\psi_i}{\Omega_r} \frac{\Omega_i}{\Omega_r} + \left(\frac{\Omega_i}{\Omega_r} \right)^2 \frac{\psi_r}{\Omega_r} \right\} \\
 & + \frac{1}{2} \frac{\beta_r}{\beta_c} X_i^{(1)} X_{ri}^{(2)} X_{iir}^{(5)} e^{-j(\theta_i^{(1)} + \theta_{ri}^{(2)} - \theta_{iir}^{(5)})} \\
 & \cdot \left\{ -j \left(\frac{\Omega_i}{\Omega_r} \right)^2 \frac{\psi_r}{\Omega_r} + \frac{\Omega_i}{\Omega_r} \frac{\psi_i}{\Omega_r} - j \frac{\Omega_i}{\Omega_r} \frac{\psi_i}{\Omega_r} + \left(\frac{\psi_i}{\Omega_r} \right)^2 \frac{\psi_r}{\Omega_r} \right\} \\
 & + \frac{1}{2} \frac{\beta_i}{\beta_c} X_r^{(1)} X_{ir}^{(2)} X_{iir}^{(5)} e^{-j(\theta_r^{(1)} + \theta_{ir}^{(2)} - \theta_{iir}^{(5)})} \\
 & \cdot \left\{ -j^2 \frac{\Omega_i}{\Omega_r} \frac{\psi_i}{\Omega_r} + \left(\frac{\Omega_i}{\Omega_r} \right)^2 \frac{\psi_r}{\Omega_r} + \left(\frac{\psi_i}{\Omega_r} \right)^2 \frac{\psi_r}{\Omega_r} \right\} \\
 & + \frac{1}{2} \frac{\beta_i}{\beta_c} X_r^{(1)} X_i^{(1)} X_{iir}^{(5)} e^{-j(\theta_r^{(1)} + \theta_i^{(1)} - \theta_{iir}^{(5)})}
 \end{aligned}$$

(P Contd.)

$$\begin{aligned}
 & \cdot \left\{ -\frac{j}{2} \left(\frac{\psi_i}{\Omega_r} \right)^2 \frac{\psi_r}{\Omega_r} + \frac{1}{2} \frac{\psi_i}{\Omega_r} \frac{\Omega_i}{\Omega_r} + \left(\frac{\Omega_i}{\Omega_r} \right)^2 \frac{\psi_r}{\Omega_r} \right\} \\
 & + j \frac{\beta_r}{\beta_c} \frac{\psi_i}{\Omega_r} \frac{\Omega_i}{\Omega_r} X_r^{(1)} X_i^{(1)} X_{ii}^{(3)} e^{-j\theta_r^{(1)}} \left\{ \cos(\theta_i^{(1)} - \theta_{ii}^{(3)}) - \frac{\beta_r}{\beta_i} \sin(\theta_i^{(1)} - \theta_{ii}^{(3)}) \right\} \\
 & + \frac{1}{2} \frac{\beta_r}{\beta_c} X_i^{(1)} X_i^{(1)} X_{ri}^{(3)} e^{-j\theta_{ri}^{(3)}} \left\{ j \left(\frac{\Omega_i}{\Omega_r} \right)^2 \frac{\psi_r}{\Omega_r} - \frac{\Omega_i}{\Omega_r} \frac{\psi_i}{\Omega_r} \right\} \\
 & + \frac{1}{2} \frac{\beta_i}{\beta_c} \frac{\Omega_i}{\Omega_r} X_r^{(1)} X_i^{(1)} X_{ir}^{(3)} e^{-j(\theta_r^{(1)} + \theta_i^{(1)} - \theta_{ir}^{(3)})} \left\{ j \frac{\psi_i}{\Omega_r} + \frac{\Omega_i}{\Omega_r} \frac{\psi_r}{\Omega_r} \right\} \\
 & - \frac{j}{2} \frac{\beta_r}{\beta_c} \frac{\Omega_i}{\Omega_r} X_i^{(1)} X_i^{(1)} X_{ri}^{(2)} e^{-j\theta_{ri}^{(2)}} \left\{ j \frac{\psi_i}{\Omega_r} + \frac{\Omega_i}{\Omega_r} \frac{\psi_r}{\Omega_r} \right\} \\
 & - \frac{j}{2} \frac{\beta_i}{\beta_c} \frac{\Omega_i}{\Omega_r} X_r^{(1)} X_i^{(1)} X_{ir}^{(2)} e^{-j(\theta_r^{(1)} - \theta_i^{(1)} + \theta_{ir}^{(2)})} \left\{ j \frac{\psi_r}{\Omega_r} \frac{\Omega_i}{\Omega_r} + \frac{\psi_i}{\Omega_r} \right\} \\
 & + j \left(1 + \frac{\beta_i}{\beta_r} \right) \left\{ \frac{j}{2} \left(1 + \frac{\beta_i}{\beta_r} \right) \frac{\Omega_i}{\Omega_r} \frac{\psi_i}{\Omega_r} \frac{\beta_r}{\beta_c} \frac{\beta_r}{\beta_i} X_r^{(1)} X_i^{(1)} X_i^{(1)} e^{-j\theta_r^{(1)}} \right. \\
 & + \frac{1}{2} \frac{\beta_r}{\beta_c} \frac{\beta_r}{\beta_i} \frac{\psi_i}{\Omega_r} X_i^{(1)} X_i^{(1)} X_{ri}^{(2)} e^{-j\theta_{ri}^{(2)}} \left(-j \frac{\Omega_i}{\Omega_r} + \frac{\psi_i}{\Omega_r} \frac{\psi_r}{\Omega_r} \right) \\
 & \left. + \frac{1}{2} \frac{\beta_r}{\beta_c} \frac{\psi_i}{\Omega_r} X_r^{(1)} X_i^{(1)} X_{ir}^{(2)} e^{j(\theta_i^{(1)} - \theta_r^{(1)} - \theta_{ir}^{(2)})} \left(-j \frac{\Omega_i}{\Omega_r} + \frac{\psi_i}{\Omega_r} \frac{\psi_r}{\Omega_r} \right) \right\}
 \end{aligned}$$

(P Contd.)

$$\begin{aligned}
 & + j \left(1 - \frac{\beta_i}{\beta_r} \right) \left\{ \frac{j}{2} \left(1 - \frac{\beta_i}{\beta_r} \right) \frac{\beta_r}{\beta_c} \frac{\beta_r}{\beta_i} \frac{\Omega_i}{\Omega_r} \frac{\psi_i}{\Omega_r} X_r^{(1)} X_i^{(1)} X_i^{(1)} e^{-j\theta_r^{(1)}} \right. \\
 & + \frac{1}{2} \frac{\beta_r}{\beta_c} \frac{\beta_r}{\beta_i} \frac{\psi_i}{\Omega_r} X_i^{(1)} X_i^{(1)} X_{ri}^{(3)} e^{-j\theta_{ri}^{(3)}} \left(-j \frac{\Omega_i}{\Omega_r} + \frac{\psi_i}{\Omega_r} \frac{\psi_r}{\Omega_r} \right) \\
 & \left. + \frac{1}{2} \frac{\beta_r}{\beta_c} \frac{\psi_i}{\Omega_r} X_r^{(1)} X_i^{(1)} X_{ir}^{(3)} e^{j(-\theta_r^{(1)} - \theta_i^{(1)} + \theta_{ir}^{(3)})} \left(j \frac{\Omega_i}{\Omega_r} + \frac{\psi_i}{\Omega_r} \frac{\psi_r}{\Omega_r} \right) \right\} \Bigg] ,
 \end{aligned}$$

$$\begin{aligned}
 S & = \frac{1}{16} \frac{\beta_r}{\beta_c} \left[2 \frac{\psi_i}{\Omega_r} \frac{\psi_r}{\Omega_r} \frac{\Omega_i}{\Omega_r} X_i^{(1)} X_r^{(1)} X_{ii}^{(3)} e^{-j\theta_r^{(1)}} \right. \\
 & \cdot \left\{ \cos (\theta_i^{(1)} - \theta_{ii}^{(3)}) - \sin (\theta_i^{(1)} - \theta_{ii}^{(3)}) \right\} \\
 & + \frac{\beta_r}{\beta_i} \frac{\psi_i}{\Omega_r} X_i^{(1)} X_i^{(1)} X_{ri}^{(3)} e^{-j\theta_r^{(3)}} \left\{ \frac{\psi_r}{\Omega_r} \frac{\Omega_i}{\Omega_r} + j \frac{\psi_i}{\Omega_r} \right\} \\
 & - j \frac{\psi_i}{\Omega_r} X_r^{(1)} X_i^{(1)} X_{ir}^{(3)} e^{-j(\theta_r^{(1)} + \theta_i^{(1)} - \theta_{ir}^{(3)})} \left\{ \frac{\psi_r}{\Omega_r} \frac{\Omega_i}{\Omega_r} + j \frac{\psi_i}{\Omega_r} \right\} \\
 & + \frac{\beta_r}{\beta_i} \frac{\psi_i}{\Omega_r} X_i^{(1)} X_i^{(1)} X_{ri}^{(2)} e^{-j(2\theta_i^{(1)} + \theta_{ri}^{(2)})} \left\{ \frac{\psi_r}{\Omega_r} \frac{\Omega_i}{\Omega_r} + j \frac{\psi_i}{\Omega_r} \right\} \\
 & + \frac{\psi_i}{\Omega_r} X_r^{(1)} X_i^{(1)} X_{ir}^{(2)} e^{-j(\theta_r^{(1)} + \theta_i^{(1)} + \theta_{ir}^{(2)})} \left\{ \frac{\psi_i}{\Omega_r} + j \frac{\psi_r}{\Omega_r} \frac{\Omega_i}{\Omega_r} \right\} \\
 & \left. + j \frac{\beta_r}{\beta_i} \left(\frac{\psi_i}{\Omega_r} \right)^2 X_r^{(1)} X_i^{(1)} X_i^{(1)} e^{-j\theta_r^{(1)}} \right] ,
 \end{aligned}$$

$$T = \frac{3}{16} \frac{\beta_r}{\beta_c} \frac{\beta_r}{\beta_i} \left(\frac{\psi_i}{\Omega_r} \right)^2 \frac{\psi_r}{\Omega_r} X_i^{(1)} X_i^{(1)} X_r^{(1)} e^{-j\theta_r^{(1)}}$$

The output at the second harmonic frequency $2f_r$ is given by

$$\begin{aligned} \frac{V_{2f_r}}{V_{inr}} &= \frac{1}{4} \sqrt{\frac{P_{inr}}{I_o V_o}} \left(\frac{V'_r}{V_{inr}} \right)^2 \left(\frac{D_{2r}}{D_r} \right)^2 \sqrt{\frac{\beta_r}{\beta_c}} \frac{\Omega_r}{\psi_{2r}} \sqrt{\frac{\Omega_r}{\psi_r}} \\ &\cdot \frac{1 + D_{2r} b_{2r} - jD_{2r} d_{2r}}{j\delta_r - b_{2r} + jd_{2r}} e^{2\zeta_r \delta_r} \left[\frac{\psi_{2r}}{\Omega_{2r}} \left\{ X_r^{(1)} X_r^{(1)} e^{-2j\theta_r^{(1)}} \left(2 \left(\frac{\psi_r}{\Omega_r} \right)^2 - 1 \right) \right. \right. \\ &+ X_r^{(1)} X_{rr}^{(2)} e^{-j(\theta_r^{(1)} + \theta_{rr}^{(2)})} \left. \left. \left(1 + j \left(\frac{\psi_r}{\Omega_r} \right)^2 \right) \right\} \right. \\ &+ \left. \frac{\psi_r}{\Omega_r} \left\{ jX_r^{(1)} X_r^{(1)} e^{-2j\theta_r^{(1)}} + (1 + j) X_r^{(1)} X_{rr}^{(2)} e^{-j(\theta_r^{(1)} + \theta_{rr}^{(2)})} \right\} \right] \cdot (6.11) \end{aligned}$$

The output at $2f_r - f_p$ is given by

$$\begin{aligned} \frac{V_{2f_r - f_p}}{V_{inp}} &= 4 \frac{P_{inr}}{I_o V_o} \left(\frac{V'_r}{V_{inr}} \right)^2 \frac{V'_p}{V_{inp}} \left(\frac{D_r}{D_p} \right)^2 \left(\frac{D_{2r-p}}{D_r} \right)^2 \frac{\Omega_r}{\psi_r} \frac{\Omega_r}{\Omega_{2r-p}} \\ &\frac{1 + D_{2r-p} b_{2r-p} - jD_{2r-p} d_{2r-p}}{j \left(\frac{2\delta_r}{\beta_r} + \frac{D_p}{D_r} \frac{\delta_p^*}{\beta_p} \right) - D_{2r-p} b_{2r-p} + j \frac{D_{2r-p}}{D_r} d_{2r-p}} \\ &\cdot e^{2\zeta_r \delta_r + \zeta_p \delta_p^*} \left[jU + \frac{\Omega_{2r-p}}{\psi_{2r-p}} W + \frac{1}{2} \left(2 - \frac{\beta_p}{\beta_r} \right) Y + \frac{1}{3} \left(2 - \frac{\beta_p}{\beta_r} \right)^2 Z \right], (6.12) \end{aligned}$$

where

$$\begin{aligned}
 U = & \frac{1}{16} \left[-\frac{1}{4} \left(2 - \frac{\beta_p}{\beta_r} \right)^2 \frac{\beta_r}{\beta_c} \frac{\Omega_p}{\Omega_r} X_r^{(1)} X_r^{(1)} X_p^{(1)} e^{j(\theta_p^{(1)} - 2\theta_r^{(1)})} \right. \\
 & + \frac{j}{2} \left(2 - \frac{\beta_p}{\beta_r} \right) X_r^{(1)} e^{-j\theta_r^{(1)}} \left\{ \left(-j \frac{\Omega_p}{\Omega_r} + \frac{\psi_p}{\Omega_r} \frac{\psi_r}{\Omega_r} \right) \frac{\beta_r}{\beta_c} X_p^{(1)} X_{rp}^{(3)} e^{j(\theta_p^{(1)} - \theta_{rp}^{(3)})} \right. \\
 & + \left(j \frac{\Omega_p}{\Omega_r} + \frac{\psi_p}{\Omega_r} \frac{\psi_r}{\Omega_r} \right) \frac{\beta_p}{\beta_c} X_r^{(1)} X_{pr}^{(3)} e^{-j(\theta_r^{(3)} - \theta_{pr}^{(3)})} \\
 & + \left. \left(-j + \left(\frac{\psi_r}{\Omega_p} \right)^2 \right) \frac{\Omega_p}{\Omega_r} \frac{\beta_r}{\beta_c} X_p^{(1)} X_{rr}^{(2)} e^{j(\theta_p^{(1)} - \theta_{rr}^{(2)})} \right\} \\
 & + \frac{1}{2} X_{rrp}^{(6)} e^{-j\theta_{rrp}^{(6)}} \left\{ \frac{\beta_r}{\beta_c} \left(\frac{\psi_r}{\Omega_r} \frac{\psi_r}{\Omega_r} \frac{\Omega_p}{\Omega_r} - \frac{\Omega_p}{\Omega_r} \right) X_p^{(1)} X_{rp}^{(3)} e^{j(\theta_p^{(1)} - \theta_{rp}^{(3)})} \right. \\
 & + \frac{\beta_p}{\beta_c} \left(\frac{\psi_r}{\Omega_r} \frac{\psi_p}{\Omega_r} - j \frac{\psi_r}{\Omega_r} \frac{\psi_r}{\Omega_r} \frac{\Omega_p}{\Omega_r} + \frac{\Omega_p}{\Omega_r} - j \frac{\psi_r}{\Omega_r} \frac{\psi_p}{\Omega_r} \right) X_r^{(1)} X_{pr}^{(3)} e^{-j(\theta_r^{(1)} - \theta_{pr}^{(3)})} \\
 & - j \frac{\beta_r}{\beta_c} \frac{\psi_r}{\Omega_r} \left(\frac{\psi_p}{\Omega_r} + \frac{\psi_r}{\Omega_r} \frac{\Omega_p}{\Omega_r} + 2j \frac{\psi_p}{\Omega_r} \right) X_p^{(1)} X_r^{(1)} e^{j(\theta_p^{(1)} - \theta_r^{(1)})} \left. \right\} \\
 & + \frac{1}{2} \frac{\beta_p}{\beta_c} X_r^{(1)} X_{pr}^{(5)} e^{-j(\theta_r^{(1)} - \theta_{pr}^{(5)})} \\
 & \cdot \left\{ \left(\frac{\psi_r}{\Omega_r} \frac{\psi_p}{\Omega_r} + j \frac{\psi_r}{\Omega_r} \frac{\psi_p}{\Omega_r} + \frac{\Omega_p}{\Omega_r} + j \frac{\psi_r}{\Omega_r} \frac{\psi_r}{\Omega_r} \frac{\Omega_p}{\Omega_r} \right) X_{rr}^{(2)} e^{-j\theta_{rr}^{(2)}} \right. \\
 & \left. + \frac{\beta_p}{\beta_r} \frac{\psi_r}{\Omega_r} \left(\frac{\psi_r}{\Omega_r} \frac{\Omega_p}{\Omega_r} + j \frac{\psi_p}{\Omega_r} \right) X_r^{(1)} e^{-j\theta_r^{(1)}} \right\} \left. \right],
 \end{aligned}$$

$$\begin{aligned}
 W = & \frac{1}{32} X_{rrp}^{(6)} e^{-j\theta_{rrp}^{(6)}} \left\{ \frac{\beta_r}{\beta_c} \left(-\frac{\Omega_p}{\Omega_r} + \left(\frac{\psi_r}{\Omega_r} \right)^2 \frac{\psi_p}{\Omega_r} \right) X_p^{(1)} X_{rp}^{(3)} e^{j(\theta_p^{(1)} - \theta_{rp}^{(3)})} \right. \\
 & + \frac{\beta_p}{\beta_c} \left(j \frac{\psi_p}{\Omega_r} + \frac{\psi_r}{\Omega_r} \frac{\Omega_p}{\Omega_r} + j \frac{\psi_r}{\Omega_r} \frac{\Omega_p}{\Omega_r} + \left(\frac{\psi_r}{\Omega_r} \right)^2 \frac{\psi_p}{\Omega_r} \right) X_r^{(1)} X_{pr}^{(3)} e^{-j(\theta_r^{(1)} - \theta_{pr}^{(3)})} \\
 & \left. + \frac{\beta_r}{\beta_c} \left(j \left(\frac{\psi_r}{\Omega_r} \right)^2 \frac{\psi_p}{\Omega_r} + \frac{\psi_p}{\Omega_r} + \frac{\psi_r}{\Omega_r} \frac{\Omega_p}{\Omega_r} \right) X_p^{(1)} X_r^{(1)} e^{j(\theta_p^{(1)} - \theta_r^{(1)})} \right\} \\
 & + \frac{1}{32} \frac{\beta_p}{\beta_c} X_r^{(1)} X_{rr}^{(2)} X_{pr}^{(5)} e^{-j(\theta_r^{(1)} + \theta_{rr}^{(2)} - \theta_{pr}^{(5)})} \\
 & \cdot \left\{ -j \frac{\psi_r}{\Omega_r} \frac{\Omega_p}{\Omega_r} + \frac{\psi_r}{\Omega_r} \frac{\Omega_p}{\Omega_r} - j \frac{\psi_p}{\Omega_p} + \left(\frac{\psi_r}{\Omega_r} \right)^2 \frac{\psi_p}{\Omega_p} \right\} \\
 & + \frac{1}{32} \frac{\beta_p}{\beta_c} \frac{\beta_p}{\beta_r} \frac{\psi_r}{\Omega_r} X_r^{(1)} X_r^{(1)} X_{pr}^{(5)} e^{-j(2\theta_r^{(1)} - \theta_{pr}^{(5)})} \left\{ -j \frac{\psi_r}{\Omega_r} \frac{\psi_p}{\Omega_r} + \frac{\Omega_p}{\Omega_r} \right\} \\
 & + \frac{j}{32} X_r^{(1)} e^{-j\theta_r^{(1)}} \left\{ \frac{\beta_r}{\beta_c} \left(\frac{\Omega_p}{\Omega_r} \frac{\psi_r}{\Omega_r} + j \frac{\psi_p}{\Omega_r} \right) X_p^{(1)} X_{rp}^{(3)} e^{j(\theta_p^{(1)} - \theta_{rp}^{(3)})} \right. \\
 & + \frac{\beta_p}{\beta_c} \left(\frac{\psi_p}{\Omega_r} - j \frac{\psi_r}{\Omega_r} \frac{\Omega_p}{\Omega_r} \right) X_r^{(1)} X_{pr}^{(3)} e^{-j(\theta_r^{(1)} - \theta_{pr}^{(3)})} \\
 & \left. + 2j \frac{\beta_r}{\beta_c} \frac{\psi_p}{\Omega_r} X_r^{(1)} X_p^{(1)} e^{j(-\theta_r^{(1)} + \theta_p^{(1)})} \right. \\
 & \left. + \left[2 \frac{\psi_p}{\Omega_r} \frac{\beta_r}{\beta_c} \left(-j + \left(\frac{\psi_r}{\Omega_r} \right)^2 \right) - \frac{\psi_r}{\Omega_r} \frac{\beta_p}{\beta_c} \left(j + \frac{\Omega_p}{\Omega_r} \right) \right] X_p^{(1)} X_{rr}^{(2)} e^{j(\theta_p^{(1)} - \theta_{rr}^{(2)})} \right\}
 \end{aligned}$$

(W contd.)

$$\begin{aligned}
 & + \frac{j}{32} \left(1 - \frac{\beta_p}{\beta_r} \right) \frac{\psi_r}{\Omega_r} X_r^{(1)} e^{-j\theta_r^{(1)}} \left\{ j \frac{\beta_r}{\beta_c} \left(1 - \frac{\beta_p}{\beta_r} \right) \frac{\Omega_p}{\Omega_r} X_r^{(1)} X_p^{(1)} e^{j(\theta_p^{(1)} - \theta_r^{(1)})} \right. \\
 & + \frac{\beta_r}{\beta_c} \left(-j \frac{\Omega_p}{\Omega_r} + \frac{\psi_p}{\Omega_r} \frac{\psi_r}{\Omega_r} \right) X_p^{(1)} X_{rp}^{(3)} e^{j(\theta_p^{(1)} - \theta_{rp}^{(3)})} \\
 & \left. + \frac{\beta_p}{\beta_c} \left(j \frac{\Omega_p}{\Omega_r} + \frac{\psi_p}{\Omega_r} \frac{\psi_r}{\Omega_r} \right) X_r^{(1)} X_{pr}^{(3)} e^{-j(\theta_r^{(1)} - \theta_{pr}^{(3)})} \right\} ,
 \end{aligned}$$

$$\begin{aligned}
 Y & = \frac{1}{16} \frac{\psi_r}{\Omega_r} X_r^{(1)} e^{-j\theta_r^{(1)}} \left\{ \frac{\beta_r}{\beta_c} \left(\frac{\Omega_p}{\Omega_r} \frac{\psi_r}{\Omega_r} + j \frac{\psi_p}{\Omega_r} \right) X_p^{(1)} X_{rp}^{(3)} e^{j(\theta_p^{(1)} - \theta_{rp}^{(3)})} \right. \\
 & + \frac{\beta_p}{\beta_c} \left(\frac{\psi_p}{\Omega_r} - j \frac{\Omega_p}{\Omega_r} \frac{\psi_r}{\Omega_r} \right) X_r^{(1)} X_{pr}^{(3)} e^{-j(\theta_r^{(1)} - \theta_{pr}^{(3)})} \left. \right\} \\
 & + \frac{1}{16} \frac{\beta_r}{\beta_c} \frac{\psi_p}{\Omega_r} \frac{\psi_r}{\Omega_r} X_p^{(1)} X_r^{(1)} X_{rr}^{(2)} e^{j(\theta_p^{(1)} - \theta_r^{(1)} - \theta_{rr}^{(2)})} (1 + j) \\
 & + \frac{j}{16} \frac{\psi_r}{\Omega_r} \left(\frac{\beta_r}{\beta_c} \frac{\psi_p}{\Omega_r} - \frac{1}{2} \frac{\beta_p}{\beta_c} \frac{\psi_r}{\Omega_r} \frac{\Omega_p}{\Omega_r} \right) X_r^{(1)} X_r^{(1)} X_p^{(1)} e^{j(\theta_p^{(1)} - 2\theta_r^{(1)})} ,
 \end{aligned}$$

$$Z = \frac{3}{32} \frac{\beta_r}{\beta_c} \left(\frac{\psi_r}{\Omega_r} \right)^2 \frac{\psi_p}{\Omega_r} X_r^{(1)} X_r^{(1)} X_r^{(1)} e^{j(\theta_p^{(1)} - 2\theta_r^{(1)})} .$$

$$\zeta_n = \beta_{en} D_n z = 2 \pi D_n N_n ,$$

$$X_n^{(1)} e^{-j\theta_n^{(1)}} = \frac{1}{\delta_n} ,$$

$$X_{ni}^{(2)} e^{-j\theta_{ni}^{(2)}} = \frac{1}{\delta_n + \frac{\beta_{i i} D_i}{\beta_{n n} D} \delta_i} ,$$

$$X_{ni}^{(3)} e^{-j\theta_{ni}^{(3)}} = \frac{1}{\delta_n + \frac{\beta_{i i} D_i}{\beta_{n n} D} \delta_i^*} ,$$

$$X_{nli}^{(4)} e^{-j\theta_{nli}^{(4)}} = \frac{1}{\delta_n + \frac{\beta_{l l} D_l}{\beta_{n n} D} \delta_l + \frac{\beta_{i i} D_i}{\beta_{n n} D} \delta_i} ,$$

$$X_{nli}^{(5)} e^{-j\theta_{nli}^{(5)}} = \frac{1}{\delta_n + \frac{\beta_{l l} D_l}{\beta_{n n} D} \delta_l^* + \frac{\beta_{i i} D_i}{\beta_{n n} D} \delta_i^*}$$

and

$$X_{nli}^{(6)} e^{-j\theta_{nli}^{(6)}} = \frac{1}{\delta_n + \frac{\beta_{l l} D_l}{\beta_{n n} D} \delta_l + \frac{\beta_{i i} D_i}{\beta_{n n} D} \delta_i^*} .$$

6.3 Future Work. The equations derived above give the output voltage at the input frequencies f_r up to the third-order approximation. The effect of all the input signals on one of them (cross-modulation) can be evaluated from these expressions. Expressions are also given for the output voltage at some of the generated frequencies (inter-modulation components). The equations are being programmed for numerical computation on a digital computer.

It should be noted that this analysis fails in the saturation region due to the limited number of successive approximations used. In order to describe the operation of the amplifier in the saturation region a different approach has to be used. A large-signal analysis using a Lagrangian formulation will be worked out in the next period.

7. General Conclusions (C. Yeh)

Computer results on the large-signal trajectory calculations for a d-c quadrupole amplifier operating under both the cyclotron-to-cyclotron mode and the cyclotron-to-synchronous mode have been obtained. Energy relations have also been computed. Results for these two modes of operation are compared for a certain quadrupole structure. It is found that under strong pump field operation, a cyclotron-to-synchronous mode gives high efficiency operation compared to the cyclotron-to-cyclotron mode. It is further believed that in this mode of operation, the r-f power is supplied by the pump at the expense of its d-c power.

Based upon the quantum mechanical tunneling effect in semiconductor materials, an equation expressing the V-I characteristics of a tunnel diode which include the effect of temperature, doping concentration

and bias voltage has been derived. The equation will be checked for accuracy for a typical semiconductor and, if satisfactory, will be used to compute the cross-modulation effect in multiple-input-signal operation.

General equations for the cross-modulation product of a crossed-field amplifier under multiple-input operation have been derived. The small-signal nonlinear version of this analysis is being programmed for computer calculations. Due to the additional dimension to be considered in the crossed-field operation, a new product of frequencies $f_r + f_p - f_s$ becomes important. Because of the fact that less gain per unit length of the crossed-field amplifier structure is involved, it is believed that the required accuracy to get correct results from the large-signal analysis for this type of structure is far less strict than that for the O-type TWA.

The theoretical and experimental work on cross-modulation products in an O-type traveling-wave amplifier have been terminated and a summary of the complete work in the form of a technical report will be issued soon.

DISTRIBUTION LIST

<u>No. Copies</u>	<u>Agency</u>
3	Chief, Bureau of Ships, Department of the Navy, Washington 25, D. C., Attn: Code 681A1D
1	Chief, Bureau of Ships, Department of the Navy, Washington 25, D. C., Attn: Code 681B2
1	Chief, Bureau of Ships, Department of the Navy, Washington 25, D. C., Attn: Code 687A
3	Chief, Bureau of Ships, Department of the Navy, Washington 25, D. C., Attn: Code 210L
1	Chief, Bureau of Naval Weapons, Department of the Navy, Washington 25, D. C., Attn: Code RAAV-333
1	Chief, Bureau of Naval Weapons, Department of the Navy, Washington 25, D. C., Attn: Code RAAV-61
1	Chief, Bureau of Naval Weapons, Department of the Navy, Washington 25, D. C., Attn: Code RMGA-11
1	Chief, Bureau of Naval Weapons, Department of the Navy, Washington 25, D. C., Attn: Code RMGA-81
1	Director, U. S. Naval Research Laboratory, Washington 25, D. C., Attn: Code 524
2	Director, U. S. Naval Research Laboratory, Washington 25, D. C., Attn: Code 5437
2	Commanding Officer and Director, U. S. Navy Electronics Laboratory, San Diego 52, California, Attn: Code 3260
2	Commander, Aeronautical Systems Division, U. S. Air Force, Wright-Patterson Air Force Base, Ohio, Attn: Code ASRPSV-1
2	Commanding Officer, U. S. Army Electronics Research and Development Laboratory, Electron Devices Division, Fort Monmouth, New Jersey
3	Advisory Group on Electron Devices, 346 Broadway, 8th Floor, New York 13, New York
1	Commanding General, Rome Air Development Center, Griffis Air Force Base, Rome, New York, Attn: RCUIL-2
20	Headquarters, Defense Documentation Center, For Scientific and Technical Information, U. S. Air Force, Cameron Station, Alexandria, Virginia

<u>No. Copies</u>	<u>Agency</u>
1	Microwave Electronics Corporation, 3165 Porter Drive, Stanford Industrial Park, Palo Alto, California
1	Mr. A. G. Peifer, Bendix Corporation, Research Laboratories, Northwestern Highway and 10-1/2 Mile Road, Southfield, Michigan
1	Bendix Corporation, Systems Division, 3300 Plymouth Road, Ann Arbor, Michigan, Attn: Technical Library
1	Litton Industries, 960 Industrial Road, San Carlos, California, Attn: Technical Library
1	Dr. R. P. Wadhwa, Electron Tube Division, Litton Industries, 960 Industrial Way, San Carlos, California
1	Microwave Associates, Burlington, Massachusetts, Attn: Technical Library
1	Microwave Electronic Tube Company, Inc., Salem, Massachusetts, Attn: Technical Library
1	Radio Corporation of America, Power Tube Division, Harrison, New Jersey
1	Raytheon Company, Burlington, Massachusetts, Attn: Technical Library
1	S-F-D Laboratories, 800 Rahway Avenue, Union, New Jersey, Attn: Technical Library
1	Dr. Walter M. Nunn, Jr., Electrical Engineering Department, Tulane University, New Orleans, Louisiana
1	Westinghouse Electric Corporation, P. O. Box 284, Elmira, New York, Attn: Technical Library
1	Bendix Corporation, Red Bank Division, Eatontown, New Jersey, Attn: Dr. James Palmer
1	Mr. A. Weglein, Hughes Aircraft Company, Microwave Tube Division, 11105 South LaCienega Blvd., Los Angeles 9, California
1	The University of Arizona, University Library, Tucson, Arizona
1	Eitel-McCullough, Inc., 13259 Sherman Way, North Hollywood, California, Attn: Dr. John E. Nevins, Jr.
1	Hughes Aircraft Company, Microwave Tube Division, 11105 South La Cienega Boulevard, Los Angeles 45, California, 90009, Attn: Dr. John Mendell

<p> <u>UD</u> The University of Michigan, Electron Physics Laboratory, Ann Arbor, Michigan. BASIS RESEARCH IN MICROWAVE DEVICES AND QUANTUM ELECTRONICS, by M. E. El-Shandaily, et al. May, 1965, 59 pp. Incl. 11 illus. (Project Serial No. SR0080901, Task 9391, Contract No. N00br-89274) </p> <p> Large-signal trajectory computations for a d-c quadrupole amplifier with a twisted quadrupole pump field structure are presented. Two modes of operation, the cyclotron-to-cyclotron mode and the cyclotron-to- synchronous mode are studied. The results are compared in terms of the paths of electrons for different pump field strength, source of r-f power supply and efficiency. It is believed that the cyclotron-to- synchronous mode of operation is more efficient in many respects. </p> <p> The derivation of the equation for the V-I characteristics of a tunnel diode is presented. It incorporates the effects of temperature, semiconductor material, doping concentration and the bias voltage on the negative resistance characteristic of the diode. This equation will be used to study cross-modulation effects in the tunnel diode under multiple-input-signal operation. </p> <p> A small-signal nonlinear analysis of a crossed-field amplifier with n input frequencies is derived. It is found that besides the usual cross-modulation product of frequencies $2f_x - f_y$, as in the case of O-type TWA, a new product in the form of $f_x + f_p - f_s$ becomes important. </p>	<p style="text-align: center;">UNCLASSIFIED</p> <ol style="list-style-type: none"> 1. General Introduction. 2. Study of Frequency Multiplication in Angular Propagating Circuit. 3. Analysis of Amplitude- and Phase-Modulated Traveling-Wave Amplifiers. 4. Study of a D-c Pumped Quadrupole Amplifier. 5. Investigation of the Cross-Modulation Products in a Wideband Tunnel Diode Amplifier. 6. Nonlinear Analysis of the Crossed-Field Amplifier with Multi-Signal Input. 7. General Conclusions. <p style="text-align: right;">I. El-Shandaily, M. E. II. Ho, B. III. Rowe, J. E. IV. Yeh, C.</p>	<p> <u>UD</u> The University of Michigan, Electron Physics Laboratory, Ann Arbor, Michigan. BASIS RESEARCH IN MICROWAVE DEVICES AND QUANTUM ELECTRONICS, by M. E. El-Shandaily, et al. May, 1965, 59 pp. Incl. 11 illus. (Project Serial No. SR0080901, Task 9391, Contract No. N00br-89274) </p> <p> Large-signal trajectory computations for a d-c quadrupole amplifier with a twisted quadrupole pump field structure are presented. Two modes of operation, the cyclotron-to-cyclotron mode and the cyclotron-to- synchronous mode are studied. The results are compared in terms of the paths of electrons for different pump field strength, source of r-f power supply and efficiency. It is believed that the cyclotron-to- synchronous mode of operation is more efficient in many respects. </p> <p> The derivation of the equation for the V-I characteristics of a tunnel diode is presented. It incorporates the effects of temperature, semiconductor material, doping concentration and the bias voltage on the negative resistance characteristic of the diode. This equation will be used to study cross-modulation effects in the tunnel diode under multiple-input-signal operation. </p> <p> A small-signal nonlinear analysis of a crossed-field amplifier with n input frequencies is derived. It is found that besides the usual cross-modulation product of frequencies $2f_x - f_y$, as in the case of O-type TWA, a new product in the form of $f_x + f_p - f_s$ becomes important. </p>	<p style="text-align: center;">UNCLASSIFIED</p> <ol style="list-style-type: none"> 1. General Introduction. 2. Study of Frequency Multiplication in Angular Propagating Circuit. 3. Analysis of Amplitude-Modulated Traveling-Wave Amplifiers. 4. Study of a D-c Pumped Quadrupole Amplifier. 5. Investigation of the Cross-Modulation Products in a Wideband Tunnel Diode Amplifier. 6. Nonlinear Analysis of the Crossed-Field Amplifier with Multi-Signal Input. 7. General Conclusions. <p style="text-align: right;">I. El-Shandaily, M. E. II. Ho, B. III. Rowe, J. E. IV. Yeh, C.</p>
<p> <u>UD</u> The University of Michigan, Electron Physics Laboratory, Ann Arbor, Michigan. BASIS RESEARCH IN MICROWAVE DEVICES AND QUANTUM ELECTRONICS, by M. E. El-Shandaily, et al. May, 1965, 59 pp. Incl. 11 illus. (Project Serial No. SR0080901, Task 9391, Contract No. N00br-89274) </p> <p> Large-signal trajectory computations for a d-c quadrupole amplifier with a twisted quadrupole pump field structure are presented. Two modes of operation, the cyclotron-to-cyclotron mode and the cyclotron-to- synchronous mode are studied. The results are compared in terms of the paths of electrons for different pump field strength, source of r-f power supply and efficiency. It is believed that the cyclotron-to- synchronous mode of operation is more efficient in many respects. </p> <p> The derivation of the equation for the V-I characteristics of a tunnel diode is presented. It incorporates the effects of temperature, semiconductor material, doping concentration and the bias voltage on the negative resistance characteristic of the diode. This equation will be used to study cross-modulation effects in the tunnel diode under multiple-input-signal operation. </p> <p> A small-signal nonlinear analysis of a crossed-field amplifier with n input frequencies is derived. It is found that besides the usual cross-modulation product of frequencies $2f_x - f_y$, as in the case of O-type TWA, a new product in the form of $f_x + f_p - f_s$ becomes important. </p>	<p style="text-align: center;">UNCLASSIFIED</p> <ol style="list-style-type: none"> 1. General Introduction. 2. Study of Frequency Multiplication in Angular Propagating Circuit. 3. Analysis of Amplitude- and Phase-Modulated Traveling-Wave Amplifiers. 4. Study of a D-c Pumped Quadrupole Amplifier. 5. Investigation of the Cross-Modulation Products in a Wideband Tunnel Diode Amplifier. 6. Nonlinear Analysis of the Crossed-Field Amplifier with Multi-Signal Input. 7. General Conclusions. <p style="text-align: right;">I. El-Shandaily, M. E. II. Ho, B. III. Rowe, J. E. IV. Yeh, C.</p>	<p> <u>UD</u> The University of Michigan, Electron Physics Laboratory, Ann Arbor, Michigan. BASIS RESEARCH IN MICROWAVE DEVICES AND QUANTUM ELECTRONICS, by M. E. El-Shandaily, et al. May, 1965, 59 pp. Incl. 11 illus. (Project Serial No. SR0080901, Task 9391, Contract No. N00br-89274) </p> <p> Large-signal trajectory computations for a d-c quadrupole amplifier with a twisted quadrupole pump field structure are presented. Two modes of operation, the cyclotron-to-cyclotron mode and the cyclotron-to- synchronous mode are studied. The results are compared in terms of the paths of electrons for different pump field strength, source of r-f power supply and efficiency. It is believed that the cyclotron-to- synchronous mode of operation is more efficient in many respects. </p> <p> The derivation of the equation for the V-I characteristics of a tunnel diode is presented. It incorporates the effects of temperature, semiconductor material, doping concentration and the bias voltage on the negative resistance characteristic of the diode. This equation will be used to study cross-modulation effects in the tunnel diode under multiple-input-signal operation. </p> <p> A small-signal nonlinear analysis of a crossed-field amplifier with n input frequencies is derived. It is found that besides the usual cross-modulation product of frequencies $2f_x - f_y$, as in the case of O-type TWA, a new product in the form of $f_x + f_p - f_s$ becomes important. </p>	<p style="text-align: center;">UNCLASSIFIED</p> <ol style="list-style-type: none"> 1. General Introduction. 2. Study of Frequency Multiplication in Angular Propagating Circuit. 3. Analysis of Amplitude- and Phase-Modulated Traveling-Wave Amplifiers. 4. Study of a D-c Pumped Quadrupole Amplifier. 5. Investigation of the Cross-Modulation Products in a Wideband Tunnel Diode Amplifier. 6. Nonlinear Analysis of the Crossed-Field Amplifier with Multi-Signal Input. 7. General Conclusions. <p style="text-align: right;">I. El-Shandaily, M. E. II. Ho, B. III. Rowe, J. E. IV. Yeh, C.</p>

<p>DD</p> <p>The University of Michigan, Electron Physics Laboratory, Ann Arbor, Michigan. BASIC RESEARCH IN MICROWAVE DEVICES AND QUANTUM ELECTRONICS, by M. E. El-Shanhalily, et al. May, 1965, 59 pp. Incl. Illinois. (Project Serial No. SR0080901, Task 9391, Contract No. N0bar-89274)</p> <p>Large-signal trajectory computations for a d-c quadrupole amplifier with a triated quadrupole pump field structure are presented. Two modes of operation, the cyclotron-to-cyclotron mode and the cyclotron-to-asyncronous mode are studied. The results are compared in terms of the paths of electrons for different pump field strength, source of r-f power supply and efficiency. It is believed that the cyclotron-to-asyncronous mode of operation is more efficient in many respects.</p> <p>The derivation of the equation for the V-I characteristics of a tunnel diode is presented. It incorporates the effects of temperature, semiconductor material, doping concentration and the bias voltage on the negative resistance characteristic of the diode. This equation will be used to study cross-modulation effects in the tunnel diode under multiple-input-signal operation.</p> <p>A small-signal nonlinear analysis of a crossed-field amplifier with n input frequencies is derived. It is found that besides the usual cross-modulation product of frequencies $2f_x - f_y - f_p$ as in the case of O-type TWA, a new product in the form of $f_x + f_p - f_s$ becomes important.</p>	<p>UNCLASSIFIED</p> <ol style="list-style-type: none"> 1. General Introduction. 2. Study of Frequency Multiplication in Angular Propagating Circuit. 3. Analysis of Amplitude- and Phase-Modulated Traveling-Wave Amplifiers. 4. Study of a D-c Pumped Quadrupole Amplifier. 5. Investigation of the Cross-Modulation Products in a Wideband Tunnel Diode Amplifier. 6. Nonlinear Analysis of the Crossed-Field Amplifier with Multi-Signal Input. 7. General Conclusions. <p>I. El-Shanhalily, M. E. II. Ho, B. III. Rowe, J. E. IV. Yeh, C.</p>	<p>DD</p> <p>The University of Michigan, Electron Physics Laboratory, Ann Arbor, Michigan. BASIC RESEARCH IN MICROWAVE DEVICES AND QUANTUM ELECTRONICS, by M. E. El-Shanhalily, et al. May, 1965, 59 pp. Incl. Illinois. (Project Serial No. SR0080901, Task 9391, Contract No. N0bar-89274)</p> <p>Large-signal trajectory computations for a d-c quadrupole amplifier with a triated quadrupole pump field structure are presented. Two modes of operation, the cyclotron-to-cyclotron mode and the cyclotron-to-asyncronous mode are studied. The results are compared in terms of the paths of electrons for different pump field strength, source of r-f power supply and efficiency. It is believed that the cyclotron-to-asyncronous mode of operation is more efficient in many respects.</p> <p>The derivation of the equation for the V-I characteristics of a tunnel diode is presented. It incorporates the effects of temperature, semiconductor material, doping concentration and the bias voltage on the negative resistance characteristic of the diode. This equation will be used to study cross-modulation effects in the tunnel diode under multiple-input-signal operation.</p> <p>A small-signal nonlinear analysis of a crossed-field amplifier with n input frequencies is derived. It is found that besides the usual cross-modulation product of frequencies $2f_x - f_y - f_p$ as in the case of O-type TWA, a new product in the form of $f_x + f_p - f_s$ becomes important.</p>	<p>UNCLASSIFIED</p> <ol style="list-style-type: none"> 1. General Introduction. 2. Study of Frequency Multiplication in Angular Propagating Circuit. 3. Analysis of Amplitude- and Phase-Modulated Traveling-Wave Amplifiers. 4. Study of a D-c Pumped Quadrupole Amplifier. 5. Investigation of the Cross-Modulation Products in a Wideband Tunnel Diode Amplifier. 6. Nonlinear Analysis of the Crossed-Field Amplifier with Multi-Signal Input. 7. General Conclusions. <p>I. El-Shanhalily, M. E. II. Ho, B. III. Rowe, J. E. IV. Yeh, C.</p>
<p>DD</p> <p>The University of Michigan, Electron Physics Laboratory, Ann Arbor, Michigan. BASIC RESEARCH IN MICROWAVE DEVICES AND QUANTUM ELECTRONICS, by M. E. El-Shanhalily, et al. May, 1965, 59 pp. Incl. Illinois. (Project Serial No. SR0080901, Task 9391, Contract No. N0bar-89274)</p> <p>Large-signal trajectory computations for a d-c quadrupole amplifier with a triated quadrupole pump field structure are presented. Two modes of operation, the cyclotron-to-cyclotron mode and the cyclotron-to-asyncronous mode are studied. The results are compared in terms of the paths of electrons for different pump field strength, source of r-f power supply and efficiency. It is believed that the cyclotron-to-asyncronous mode of operation is more efficient in many respects.</p> <p>The derivation of the equation for the V-I characteristics of a tunnel diode is presented. It incorporates the effects of temperature, semiconductor material, doping concentration and the bias voltage on the negative resistance characteristic of the diode. This equation will be used to study cross-modulation effects in the tunnel diode under multiple-input-signal operation.</p> <p>A small-signal nonlinear analysis of a crossed-field amplifier with n input frequencies is derived. It is found that besides the usual cross-modulation product of frequencies $2f_x - f_y - f_p$ as in the case of O-type TWA, a new product in the form of $f_x + f_p - f_s$ becomes important.</p>	<p>UNCLASSIFIED</p> <ol style="list-style-type: none"> 1. General Introduction. 2. Study of Frequency Multiplication in Angular Propagating Circuit. 3. Analysis of Amplitude- and Phase-Modulated Traveling-Wave Amplifiers. 4. Study of a D-c Pumped Quadrupole Amplifier. 5. Investigation of the Cross-Modulation Products in a Wideband Tunnel Diode Amplifier. 6. Nonlinear Analysis of the Crossed-Field Amplifier with Multi-Signal Input. 7. General Conclusions. <p>I. El-Shanhalily, M. E. II. Ho, B. III. Rowe, J. E. IV. Yeh, C.</p>	<p>DD</p> <p>The University of Michigan, Electron Physics Laboratory, Ann Arbor, Michigan. BASIC RESEARCH IN MICROWAVE DEVICES AND QUANTUM ELECTRONICS, by M. E. El-Shanhalily, et al. May, 1965, 59 pp. Incl. Illinois. (Project Serial No. SR0080901, Task 9391, Contract No. N0bar-89274)</p> <p>Large-signal trajectory computations for a d-c quadrupole amplifier with a triated quadrupole pump field structure are presented. Two modes of operation, the cyclotron-to-cyclotron mode and the cyclotron-to-asyncronous mode are studied. The results are compared in terms of the paths of electrons for different pump field strength, source of r-f power supply and efficiency. It is believed that the cyclotron-to-asyncronous mode of operation is more efficient in many respects.</p> <p>The derivation of the equation for the V-I characteristics of a tunnel diode is presented. It incorporates the effects of temperature, semiconductor material, doping concentration and the bias voltage on the negative resistance characteristic of the diode. This equation will be used to study cross-modulation effects in the tunnel diode under multiple-input-signal operation.</p> <p>A small-signal nonlinear analysis of a crossed-field amplifier with n input frequencies is derived. It is found that besides the usual cross-modulation product of frequencies $2f_x - f_y - f_p$ as in the case of O-type TWA, a new product in the form of $f_x + f_p - f_s$ becomes important.</p>	<p>UNCLASSIFIED</p> <ol style="list-style-type: none"> 1. General Introduction. 2. Study of Frequency Multiplication in Angular Propagating Circuit. 3. Analysis of Amplitude- and Phase-Modulated Traveling-Wave Amplifiers. 4. Study of a D-c Pumped Quadrupole Amplifier. 5. Investigation of the Cross-Modulation Products in a Wideband Tunnel Diode Amplifier. 6. Nonlinear Analysis of the Crossed-Field Amplifier with Multi-Signal Input. 7. General Conclusions. <p>I. El-Shanhalily, M. E. II. Ho, B. III. Rowe, J. E. IV. Yeh, C.</p>

